Asymptotic Post-buckling Analysis by Koiter's Method with a General Purpose Finite Element Code

by

Paras Mehta

Thesis submitted to the Faculty of the

Virginia Polytechnic Institute and State University

in partial fulfillment of the requirements for the degree of

Master of Science

in

Aerospace & Ocean Engineering

APPROVED:

R. Haftka

R. T. Haftka, Chairman

E R Johnson

E. R. Johnson

J. N. Reddy

J. N. Reddy

December 1990

Blacksburg, Virginia

Asymptotic Post-buckling Analysis by Koiter's Method with a General Purpose Finite Element Code

by

Paras Mehta

R. T. Haftka, Chairman

Aerospace & Ocean Engineering

(ABSTRACT)

Many structures are sensitive to initial imperfections, sometimes leading to a great decrease in buckling load. Koiter showed that the effect of initial imperfections is largely determined by the initial post-buckling behavior of the perfect structure. The present work seeks to implement Koiter's method of asymptotic post-buckling analysis on a finite element program Engineering Analysis Language (EAL).

EAL is based on engineering strain measure. It is shown via examples that the predicted post-buckling behavior of a structure for engineering strain measure is approximately same as that for Green's strain measure provided the strains are small. To characterize the post-buckling behavior by Koiter's method in the finite element form, the linear and incremental stiffness matrices are required. These matrices comprise the tangent stiffness matrix. As EAL uses the modified Newton-Raphson procedure to solve nonlinear structures, it calculates the tangent stiffness. The first and second order incremental stiffnesses are extracted by partial differentiation of the tangent stiffness using a second order central difference scheme. The linear stiffness is directly given by the EAL processor "K". These stiffnesses are then used to get the post-buckling load-displacement behavior close to the bifurcation point.

Numerical results for the initial post-buckling behavior are obtained for truss and frame structures using the Koiter's analysis procedure on EAL. It is compared to the nonlinear load-displacement behavior of the structures with small initial imperfections. The post-buckling load-displacement behavior for a knee frame is also compared to the behavior obtained experimentally by Roorda [19] and analytically by Koiter [13]. The asymptotic analysis procedure has given good asymptotic post-buckling results.

Acknowledgments

I am indebted to Dr. R. T. Haftka for the help and guidance he has given me throughout this work. I wish to thank Dr. E. R. Johnson and Dr. J. N. Reddy for serving on my committee.

I would also like to thank my Femoyer office mates for their help, support and encouragement.

Table of Contents

List of Figures

Chapter 1 : Introduction

Many structures are sensitive to imperfections, and it is well known that small imperfections can sometimes lead to a great decrease in buckling load. Koiter [1] treated this problem in general terms in the context of continuum elasticity and showed that the effect of initial imperfections is largely determined by the initial post-buckling behavior of the perfect structure.

For a structure which has a critical bifurcation point (perfect structure), three types of post-buckling paths are of particular importance as discussed by Koiter [1] and Thompson [2]. The three types of bifurcation, described as asymmetric, stable-symmetric, and unstable-symmetric, are shown in Fig. 1. In the figure lines starting from origin represent the behavior of the perfect system, while the other lines represent the behavior of imperfect systems. Also, continuous lines represent stable equilibrium paths, while broken lines represent unstable equilibrium paths.

Considering first the lines representing the perfect systems, in each case the fundamental path loses its stability at a point of bifurcation or intersection at which the path intersects a second distinct and continuous path, namely the post-buckling path. At the asymmetric point of bifurcation the post-buckling paths has a non-zero slope, and the two paths exchange stability such that only the rising post-buckling path is stable. At

the symmetric points of bifurcation the post buckled paths have zero slopes, the sign of the curvature differentiating the two cases. At the stable symmetric point of bifurcation the curvature is positive and the rising post-buckling path is stable, while at the unstable symmetric point of bifurcation the curvature is negative and the falling post-buckling path is unstable.

Consider next the lines representing the equilibrium paths of the imperfect systems. For the asymmetric point of bifurcation a negative imperfection yields a completely stable natural path corresponding to a natural loading sequence from the unloaded state, together with a completely unstable complementary path of little practical interest. In contrast, a positive imperfection yields a natural path which reaches a maximum and loses its stability (snap through point), the critical load being lower than that of the perfect system.

For the stable symmetric point of bifurcation, positive and negative imperfections have essentially similar effects, yielding continuously stable natural equilibrium paths. For the unstable symmetric point of bifurcation positive and negative imperfections likewise have essentially similar effects, yielding in this case natural equilibrium paths that lose their stability at snapping points at reduced values of the load.

Depending on the kind of post-buckling path the perfect structure has, the imperfect structure may have a lower critical load. Hence, knowledge of post-buckling behavior is of interest and importance mainly as an indication of the imperfection sensitivity of the buckling load.

Structural stability phenomenon are essentially nonlinear, with rare exceptions. But, because of the extensive computation required to predict load-displacement behavior

by these methods, practical consideration of stability usually proceeds on the basis of a linearized eigenvalue analysis. The deficiency of this approach is that the error in the predicted buckling load may be substantial, and no information is obtained about the post-buckling behavior. This necessitates the use of Koiter's and other similar methods (see Refs. [1] - [11]) which give approximate post-buckling behavior but are much more efficient than a direct nonlinear approach. Some of the problems solved by these methods can be found in Refs. [1] - [22].

Present structural analysis practices rely heavily upon matrix methods of analysis based upon finite element idealization. A primary reason for this is the facility with which the finite element approach can account for irregular variations in overall configuration, material properties, applied loadings and boundary conditions. Also, the finite element approach is broadly applicable with regard to type of structure (truss, frame, shell, etc.).

Initially Koiter's method had been applied to continuum problems only. But it is actually easier to apply to discrete systems than to continuos systems. Lang [23] and Haftka et al [3,4] have put the Koiter's method in finite element notation, but Lang uses a sequence of eigenvectors instead of Koiter's efficient alternate set.

The objective of this work is to investigate the feasibility of implementing Koiter's method on a general purpose finite element program. The finite element analysis program used here is Engineering Analysis Language (EAL) [24]. EAL is a modular system of individual analysis processors which may be used in any appropriate sequence to perform a variety of analyses. EAL has FORTRAN like commands which permit branching, testing data, looping and calling runstreams (similar to calling FORTRAN subroutines). These capabilities makes it an ideal choice for the analysis.

Chapter 2 describes Koiter's method in functional form. Chapter 3 discusses the effect of strain measures on post-buckling behavior through examples. Chapter 4 states Koiter's method in finite element form. Chapter 5 describes the procedure used to get stiffness matrices by EAL and the matrices are compared to those obtained for Green's strain. Results obtained for examples solved by EAL are shown in Chapter 6.

Chapter 2 : Koiter's Method in Functional Form

Koiter's method applies the principle of minimum potential energy to derive asymptotic approximations for the initial post-buckling behavior and imperfection sensitivity of structures.

It is applicable only to structures that exhibit a bifurcation-point type of buckling. This mode of buckling is usually associated with a structure which is symmetric both in geometry and in the applied load system. This type of structure is often referred to as a perfect structure. The applied load system is assumed proportional to a single non-negative load parameter λ. For small values of λ, the displacements of the structure are continuous functions of λ and the symmetry is preserved in the deformed structure. As λ increases, a critical point is reached at which asymmetric displacements become possible, i.e. a bifurcation of the load- displacement behavior occurs at the critical point.

The load-displacement curve emanating from the origin is called the fundamental equilibrium path. In general, the lowest critical point on this fundamental equilibrium

path may result from an intersection with a multiplicity of other equilibrium paths simultaneously, and Koiter's method can account for this circumstance [8,12]. However, consideration of this complexity is omitted in this investigation. This constitutes a restriction to "simple" bifurcation points. Simple bifurcation points are assumed to arise from the fundamental equilibrium path intersecting a single equilibrium path referred to as the post-buckling equilibrium path.

A prerequisite to the use of this method is the determination of the fundamental equilibrium path of the perfect structure U, as a function of the applied load parameter λ. Starting with knowledge of the fundamental path, the first part of Koiter's analysis is initiated by looking for a critical point on that path. Stability is equated with a strict minimum of the potential energy. This means that if $U(\lambda) + u$ is any kinematically admissible state adjacent to $U(\lambda)$, then for stability, given any nontrivial u,

$$\Pi[U(\lambda) + u] - \Pi[U(\lambda)] \equiv P(u) > 0 \tag{2.1}$$

where Π denotes the total potential energy functional.

The transition energy functional $P(u)$ is expanded in a Taylor series about the fundamental equilibrium path, $u = 0$. A critical point is one where the quadratic terms of $P(u)$ or, equivalently, the second variation of $\Pi(u)$, become positive semidefinite. This critical point may be either a limit point or a bifurcation point and, in the latter case, the structure may be stable, neutral, or unstable depending upon the higher order terms in the expansion of $P(u)$. These higher order terms are systematically examined to obtain an approximation to the post-buckling equilibrium path.

The second part of Koiter's method reaches out to consider a class of structures which differ slightly from the original. The difference or "imperfection" that determines this

class usually destroys the symmetry of the structure, and the asymmetric structures do not have bifurcation points; they are "imperfect". Nevertheless, the results of the first part of the Koiter method can be readily corrected to account for the imperfection effects. This is not considered here and it is assumed that the given structure is a perfect structure.

The principal virtue of this method of analysis is that, after the fundamental equilibrium path has been determined, the remaining nonlinear problem is transformed into a sequence of linear problems. Because the interest is confined to the region of the buckling load, the nonlinear analysis is reduced to an effort equivalent to one or two linear analyses. This is slightly more effort than a linearized stability analysis and is far less effort than a direct nonlinear behavior analysis.

Fidelity to the notation of Koiter's PhD dissertation [1] is maintained in order that results from that source may be used without repeating the underlying derivations.

Let U represent the set of displacement functions and displacement function derivatives that appear in the total potential energy functional $\Pi(U)$ for a given structure and applied loading. The functional $\Pi(U)$ is expressed as a sum of functionals $\Pi_i(U)$, each of which is homogeneous of degree i in the components of U, i.e.,

$$\Pi(U) = \Pi_0(U) + \Pi_1(U) + \Pi_2(U) + \ldots \tag{2.2}$$

where, for any scalar a,

$$\Pi_i(aU) = a^i \Pi_i(U) \qquad i = 0,1,2,\ldots \tag{2.3}$$

Extending this symbolic notation, the bilinear functional Π_{11} is defined by

$$\Pi_2(U+V) = \Pi_2(U) + \Pi_{11}(U,V) + \Pi_2(V) \tag{2.4}$$

For example $\Pi_2(U) \equiv cU^2$ yields $\Pi_{11}(U,V) = 2cUV$. This notation is generalized to define functionals in several variables.

Each functional is of homogeneous degree in the variables as indicated by the subscripts. Thus $\Pi_{21}(U,V)$ is comprised of cubic terms which are second degree in the components of U and of first degree in V.

The equations of equilibrium can be derived by setting the first variation of the total potential energy of Eq. (2.2) equal to zero. Thus the variational equation is

$$0 = \Pi_1(\delta U) + \Pi_{11}(\delta U,U) + \Pi_{12}(\delta U,U) + \Pi_{13}(\delta U,U) + \ldots \tag{2.5}$$

All functionals, beyond the first two, contribute terms that are nonlinear in the components of U to the equilibrium equation.

Application of Koiter's method requires knowledge of the solution of the equilibrium equations, with boundary conditions, as a function of λ, for λ increasing from zero. In general, such a solution is difficult to obtain; on the other hand, linearization of Eq. (2.5) gives the form

$$0 = \Pi_1(\delta U) + \Pi_{11}(\delta U,U) \tag{2.6}$$

that readily admits a solution of the form

$$U(\lambda) \equiv \lambda U_0 \tag{2.7}$$

where U_0 is the solution of Eq. (2.6) for the unit load system. The derivation in this thesis is limited to the case where the fundamental path is linear or approximately linear so that Eq. (2.7) can be used.

In order to calculate the bifurcation buckling load of the structure the potential energy $P(u)$ of transition from the fundamental state to an adjacent state as defined by Eq. (2.1) is

$$P(u) = \Pi(\lambda U_0 + u) - \Pi(\lambda U_0) \tag{2.8}$$

Use of a Taylor series expansion yields this transition energy as a sum of functionals of homogeneous order.

$$P(u) = P_1(u) + P_2(u) + P_3(u) + \ldots \tag{2.9}$$

where the homogeneous functionals $P_i(u)$ may be expressed as

$$P_1(u) = 0 = \Pi_1(u) + \Pi_{11}(u,\lambda U_0) \tag{2.10}$$

$$P_2(u) = \Pi_2(u) + \Pi_{21}(u,\lambda U_0) + \Pi_{22}(u,\lambda U_0) + \ldots \tag{2.11}$$

$$P_3(u) = \Pi_3(u) + \Pi_{31}(u,\lambda U_0) + \Pi_{32}(u,\lambda U_0) + \ldots \tag{2.12}$$

$$P_4(u) = \Pi_4(u) + \Pi_{41}(u,\lambda U_0) + \Pi_{42}(u,\lambda U_0) + \ldots \tag{2.13}$$

etc.

It is assumed that the kinematic boundary conditions are homogeneous. Consequently, if some suitably normalized u is kinematically admissible, so also is au in

which a is any scalar. Substituting au for u in the transition energy functional of Eq. (2.9) yields

$$P(au) = aP_1(u) + a^2P_2(u) + a^3P_3(u) + a^4P_4(u) + \ldots \tag{2.14}$$

A sufficient condition for stability is that this potential energy functional be strictly positive for all possible kinematically admissible displacements satisfying $0 < |a| < k$ where k is a positive constant. Applying this stability criterion to Eq. (2.14) gives the necessary conditions

$$P_1(\mathring{u}) = 0 \tag{2.15}$$

$$P_2(u) \geq 0 \tag{2.16}$$

The first of these conditions is identically satisfied, as indicated in Eq. (2.10), because it simply states the condition for equilibrium of the fundamental state.

It has been shown by Koiter that, the sufficient conditions for stability are Eq. (2.15) and

$$P_2(u) > 0 \tag{2.17}$$

The functional $P_2(u)$ is a positive definite quadratic form in u for sufficiently small values of λ as the parameter is increased from zero. As λ is increased, a critical level may be reached at which the functional $P_2(u)$ becomes positive semidefinite, thereby signalling a potential loss of stability. At this critical load level $P_2(u)$ vanishes for u which satisfies

$$P_{11}(\delta u, u) = 0 \tag{2.18}$$

where δu is a kinematically admissible but otherwise arbitrary displacement field.

Using Eq. (2.11), Eq. (2.18) is written equivalently as

$$0 = \Pi_{11}(\delta u,u) + \Pi_{111}(\delta u,u,\lambda U_0) + \Pi_{112}(\delta u,u,\lambda U_0) + \ldots \tag{2.19}$$

Equation (2.19) takes the form of a nonlinear eigenvalue problem for which nontrivial solutions exist at certain discrete values of the load intensity parameter λ. Herein, it is assumed that the lowest eigenvalue $\lambda = \lambda_1$ has a unique eigenfunction $u = u_1$.This assumption of a unique buckling mode constitutes a restriction to structures with simple bifurcation points.

At the bifurcation point the structure is neutrally stable to the extent that the stability cannot be assessed by the conditions of Eqs. (2.15) and (2.16). In order to apply the stability criterion on the energy functional of Eq. (2.14), it is necessary to examine the higher order terms to obtain additional stability conditions. As $P_1(u_1) = P_2(u_1) = 0$ at the bifurcation point, observation of Eq. (2.14) leads to two additional necessary conditions:

$$P_3(u_1) = 0 \tag{2.20}$$

$$P_4(u_1) \geq 0 \tag{2.21}$$

Should the equality be satisfied in Eq. (2.21) it would again be required to seek conditions on the basis of the next higher order terms, and so on. This is not considered in this investigation.

In the following, the results obtained by Koiter for the post-buckling behavior of a perfect structure are summarized.

The equilibrium states of the structure for loads in the neighborhood of the buckling load are approximated by expansion of the potential energy about the bifurcation point. From Eqs. (2.8) and (2.9) and with use of the prime (′) to denote differentiation with respect to the load, we obtain

$$\begin{aligned}\Pi(U,\lambda) &= \Pi(\lambda, U_0) + P(u,\lambda) \\ &= \Pi(\lambda, U_0) \\ &\quad + P_2(u) + (\lambda - \lambda_1)P_2'(u) + (\lambda - \lambda_1)^2 P_2''(u) + \ldots \\ &\quad + P_3(u) + (\lambda - \lambda_1)P_3'(u) + (\lambda - \lambda_1)^2 P_3''(u) + \ldots \\ &\quad + P_4(u) + (\lambda - \lambda_1)P_4'(u) + (\lambda - \lambda_1)^2 P_4''(u) + \ldots \\ &\quad \textit{etc.}\end{aligned} \tag{2.22}$$

The Euler equations of this potential energy functional are sought in two stages by taking

$$u = a u_1 + \bar{u} \tag{2.23}$$

first, a is held constant and $\bar{u}$ is determined. Then, the remaining single degree of freedom problem in a is solved to complete the behavior analysis. Upon substitution of Eq. (2.23) into Eq. (2.22) to obtain the energy functional in terms of the chosen unknown field $\bar{u}$ it becomes necessary to truncate the energy functional expansion in order to find a solution. Moreover, the nonlinearity of the Euler equations for $\bar{u}$

necessitates the approximation of this unknown field by a series expansion. This derivation is presented in detail in Koiter's dissertation. The resulting solution for $\bar{u}$ is

$$\bar{u} = \phi_1' a(\lambda - \lambda_1) + \phi_2 a^2 \tag{2.24}$$

in which terms cubic and higher [i.e., $a^i(\lambda - \lambda_1)^j$, *for* $i + j \geq 3$] have been neglected. The associated single degree of freedom potential energy functional is given by

$$\begin{aligned} P(a) = {} & A_2'(\lambda - \lambda_1)a^2 + A_2''(\lambda - \lambda_1)^2 a^2 \\ & + A_3 a^3 + A_3'(\lambda - \lambda_1)a^3 \\ & + A_4 a^4 \end{aligned} \tag{2.25}$$

where

$$A_2' = P_2'(u_1) \tag{2.26}$$

$$A_2'' = P_2''(u_1) - P_2(\phi_1') \tag{2.27}$$

$$A_3 = P_3(u_1) \tag{2.28}$$

$$A_3' = P_3'(u_1) - P_{11}(\phi_1', \phi_2) \tag{2.29}$$

$$A_4 = P_4(u_1) - P_2(\phi_2) \tag{2.30}$$

and the unknown fields ϕ_1' and ϕ_2 are defined by the linear relations given below:

$$P_{11}(\phi_1', \delta u) + P_{11}'(u_1, \delta u) - \frac{P_2'(u_1)}{T_2(u_1)} T_{11}(u_1, \delta u) = 0 \tag{2.31}$$

$$T_{11}(u_1, \phi_1') = 0 \tag{2.32}$$

$$P_{11}(\phi_2, \delta u) + P_{21}(u_1, \delta u) - \frac{3P_3(u_1)}{2T_2(u_1)} T_{11}(u_1, \delta u) = 0 \tag{2.33}$$

$$T_{11}(u_1, \phi_2) = 0 \tag{2.34}$$

δu is an arbitrary kinematically admissible displacement state, and the functional T_2 is an arbitrary, positive definite quadratic functional. It is used for defining orthogonality of displacement fields, but its choice does not affect the final results.

Equation (2.25), evaluated at the critical load, gives us sufficient conditions for the stability of equilibrium at the critical point.

$$P(a) = A_3 a^3 + A_4 a^4 \tag{2.36}$$

Thus, the sufficient conditions for stability follow from the stability criterion of Eq. (2.1) as,

$$A_3 = 0 \tag{2.37}$$

$$A_4 > 0 \tag{2.38}$$

These sufficient conditions for stability at the critical point are the counterpart of the necessary conditions of Eqs. (2.20) and (2.21). The case $A_4 = 0$ is neutrally stable to the extent that can be determined without using higher order terms.

Equation (2.25) is typically further approximated as

$$P(a) = A_2'(\lambda - \lambda_1)a^2 + A_3a^3 + A_4a^4 \tag{2.39}$$

The states of equilibrium are characterised by stationary values of Eq. (2.39), i.e. by

$$\frac{dP(a)}{da} = 2(\lambda - \lambda_1)A_2'a + 3A_3a^2 + 4A_4a^3 = 0 \tag{2.40}$$

Hence, the load

$$\frac{\lambda}{\lambda_1} = 1 + \hat{a}a + \hat{b}a^2 \tag{2.41}$$

where, the postbuckling coefficients are

$$\hat{a} = -\frac{3A_3}{2A_2'\lambda_1} \tag{2.42}$$

$$\hat{b} = -\frac{2A_4}{A_2'\lambda_1} \tag{2.43}$$

For an asymmetric bifurcating structure, only $\hat{a}$ is calculated. For a symmetric bifurcating structure $\hat{a} = 0$ and one has to calculate $\hat{b}$ to get the post-buckling behavior.

Chapter 3 : Strain Measures and Post-buckling Behavior

In the following chapters we discuss the calculation of asymptotic postbuckling behavior via the EAL finite element program. EAL is based on a corotational formulation limited to small strains. The finite element formulation described in Chapter 4, however, is based on Green's strain which is an objective strain measure for large strains. But for small strains, the Green's strain and the Engineering strain measures are almost same. The following examples show that the two strain measures can predict widely different asymptotic post-buckling coefficients $\hat{a}$ and $\hat{b}$. However, it is also shown that the postbuckling behavior is still very close for small strains, even with the different postbuckling coefficients.

3.1 One Degree of Freedom Model

The spring bar structure shown in Fig. 2 is a popular classroom example [25,26] of a structure with asymmetric post-buckling behavior. The total potential for the spring bar structure, assuming rigid bars is

$$\Pi = \frac{1}{2} K l_s^2 \varepsilon^2 - \lambda \Delta \tag{3.1}$$

where

K	spring stiffness
l_s	initial length of the spring
ε	strain in the spring
λ	load parameter
Δ	displacement of load

The initial length of the spring is

$$l_s = \sqrt{2}\, l(1 + \sin \theta_0)^{1/2} \tag{3.2}$$

where

l	length of the rigid bars
θ_0	imperfection angle

The length of the spring after the load is applied is

$$l_f = \sqrt{2}\, l(1 + \sin \theta)^{1/2} \tag{3.3}$$

The distance through which the load moves is

$$\Delta = 2l\,(\cos\theta_0 - \cos\theta) \tag{3.4}$$

The equilibrium equation is given by equating the first variation of the total potential to zero.

$$Kl_s^2\varepsilon\frac{\partial\varepsilon}{\partial\theta} - \lambda\frac{\partial\Delta}{\partial\theta} = 0 \tag{3.5}$$

This being a simple example, we directly solve the nonlinear equilibrium equation, instead of using Koiter's method. The load displacement behavior is evaluated for different measures of strain.

3.1.1 Green's Strain

Green's strain for the spring is

$$\varepsilon = \frac{1}{2}\frac{l_f^2 - l_s^2}{l_s^2} \tag{3.6}$$

$$= \frac{\sin\theta - \sin\theta_0}{2(1+\sin\theta_0)} \tag{3.7}$$

For the imperfect model, the equilibrium load is (from Eqs. (3.2), (3.4), (3.5), (3.7))

$$\lambda = \frac{Kl}{4}\frac{(\sin\theta - \sin\theta_0)}{(1+\sin\theta_0)}\cot\theta \tag{3.8}$$

For the perfect structure

$$\theta_0 = 0 \tag{3.9}$$

Hence, for a perfect model the equilibrium load for the post-buckled path is

$$\lambda = \frac{KI}{4}\cos\theta \tag{3.10}$$

$$\simeq \frac{KI}{4}\left(1 - \frac{\theta^2}{2} + \ldots\right) \tag{3.11}$$

which corresponds to unstable symmetric post-buckling.

3.1.2 Engineering Strain

The engineering strain for the spring is

$$\varepsilon = \frac{l_f - l_s}{l_s} \tag{3.12}$$

$$= \left(\frac{1+\sin\theta}{1+\sin\theta_0}\right)^{1/2} - 1 \tag{3.13}$$

Hence, the equilibrium load for the imperfect model is (from Eqs. (3.2), (3.4), (3.5), (3.13))

$$\lambda = \frac{KI}{2}\left\{1 - \left(\frac{1+\sin\theta_0}{1+\sin\theta}\right)^{1/2}\right\}\cot\theta \tag{3.14}$$

For the perfect model, the load displacement relation after bifurcation is

$$\lambda = \frac{KI}{2}\{1-(1+\sin\theta)^{-1/2}\}\cot\theta \tag{3.15}$$

$$\simeq \frac{KI}{4}(1-\frac{3}{4}\theta+\frac{1}{8}\theta^2+...) \tag{3.16}$$

Comparing Eq. (3.16) to Eq. (3.11) we note that the nature of the postbuckling has changed from symmetric to asymmetric. However in the small strain region ($\varepsilon < 0.01$) this difference does not substantially change the load displacement curve. The load displacement plots of the model for the two strain measures are shown in Fig. 3. It can be seen that in the small strain region ($\varepsilon < 0.01$ for $\theta < 1.15^{\circ}$ for perfect structure) the plots are almost same for the two strain measures.

3.2 Two Degrees of Freedom Model

The structure shown in Fig. 4 is considered to illustrate the application of Koiter's method. The total potential for the structure, assuming rigid bars is

$$\Pi = \frac{1}{2}Kl_s^2\varepsilon_1^2 + \frac{1}{2}Kl_s^2\varepsilon_2^2 - \lambda\Delta \tag{3.17}$$

where

K	spring stiffnesses
l_s	initial length of the springs
ε_1, ε_2	strain in the springs
λ	load parameter
Δ	displacement of load

The increase in the length of the springs after the load is applied is

$$\delta_1 = l \sin\theta \tag{3.18}$$

$$\delta_2 = l \sin\chi \tag{3.19}$$

where

l	length of the rigid bars
θ, χ	rotational degrees of freedom

The distance through which the load moves is

$$\Delta = l\{3 - \cos\theta - \cos\chi - [1 - (\frac{\delta_2}{l} - \frac{\delta_1}{l})^2]^{\frac{1}{2}}\} \tag{3.20}$$

The equilibrium equation is given by equating the first variation of the total potential to zero.

$$Kl_s^2(\varepsilon_1 \frac{\partial\varepsilon_1}{\partial\theta} + \varepsilon_2 \frac{\partial\varepsilon_2}{\partial\theta}) - \lambda \frac{\partial\Delta}{\partial\theta} = 0 \tag{3.21}$$

$$Kl_s^2(\varepsilon_1 \frac{\partial\varepsilon_1}{\partial\chi} + \varepsilon_2 \frac{\partial\varepsilon_2}{\partial\chi}) - \lambda \frac{\partial\Delta}{\partial\chi} = 0 \tag{3.22}$$

The load displacement behavior is again evaluated for the two measures of strain.

3.2.1 Green's Strain

Green's strain in the springs is

$$\varepsilon_1 = \frac{\delta_1}{l_s} + \frac{1}{2}\frac{\delta_1^2}{l_s^2} \tag{3.23}$$

$$\varepsilon_2 = \frac{\delta_2}{l_s} + \frac{1}{2}\frac{\delta_2^2}{l_s^2} \tag{3.24}$$

From Eqs. (3.18) to (3.24), neglecting fourth and higher order terms, the nonlinear equilibrium equations are

$$Kl\{\theta + \frac{3l}{2l_s}\theta^2 + (-\frac{2}{3} + \frac{1}{2}\frac{l^2}{l_s^2})\theta^3\}$$

$$-\lambda\{2\theta - \chi - \frac{1}{3}\theta^3 - \theta^2\chi + \frac{3}{2}\theta\chi^2 - \frac{1}{3}\chi^3\} = 0 \tag{3.25}$$

$$Kl\{\chi + \frac{3l}{2l_s}\chi^2 + (-\frac{2}{3} + \frac{1}{2}\frac{l^2}{l_s^2})\chi^3\}$$

$$-\lambda\{-\theta + 2\chi - \frac{1}{3}\theta^3 + \frac{3}{2}\theta^2\chi - \theta\chi^2 - \frac{1}{3}\chi^3\} = 0 \tag{3.26}$$

Linearizing the equilibrium Eqs. (3.25), (3.26)

$$(Kl - 2\lambda)\theta + \lambda\chi = 0 \tag{3.27}$$

$$\lambda\theta + (Kl - 2\lambda)\chi = 0 \tag{3.28}$$

For unit load ($\lambda = 1$) the above two linearized equilibrium equations are satisfied by

$$U_0 \equiv \begin{Bmatrix} \theta_0 \\ \chi_0 \end{Bmatrix} = \begin{Bmatrix} 0 \\ 0 \end{Bmatrix} \tag{3.29}$$

Hence, the fundamental state for any load is

$$U(\lambda) \equiv \lambda U_0 = \begin{Bmatrix} 0 \\ 0 \end{Bmatrix} \tag{3.30}$$

The potential energy P(u) of transition from the fundamental state to an adjacent state is given by Eq. (3.9), where

$$P_1(u) = \Pi_1(u) = 0 \tag{3.31}$$

$$P_2(u) = \Pi_2(u) = \frac{1}{2} KI^2(\theta^2 + \chi^2) - \lambda I(\theta^2 + \chi^2 - \theta\chi) \tag{3.32}$$

$$P_3(u) = \Pi_3(u) = \frac{1}{2} K \frac{I^3}{I_s} (\theta^3 + \chi^3) \tag{3.33}$$

$$P_4(u) = \Pi_4(u) = -\frac{1}{6} KI^2 (1 - \frac{3I^2}{4I_s{}^2})(\theta^4 + \chi^4)$$

$$+ \frac{\lambda I}{12} (\theta^4 + 4\theta^3\chi - 9\theta^2\chi^2 + 4\theta\chi^3 + \chi^4) \tag{3.34}$$

$$u \equiv \begin{Bmatrix} \theta \\ \chi \end{Bmatrix} \tag{3.35}$$

At the critical point

$$P_{11}(\delta u, u) = \{(KI^2 - 2\lambda I)\theta + \lambda I\chi\}\delta\theta + \{\lambda I\theta + (KI^2 - 2\lambda I)\chi\}\delta\chi = 0 \tag{3.36}$$

Since $\delta\theta$, $\delta\chi$ are arbitrary

$$(KI^2 - 2\lambda I)\theta + \lambda I\chi = 0 \tag{3.37}$$

$$\lambda I\theta + (KI^2 - 2\lambda I)\chi = 0 \tag{3.38}$$

Solving the above two equations gives the buckling load and mode as

$$\lambda_1 = \frac{KI}{3} \tag{3.39}$$

$$u_1 \equiv \begin{Bmatrix} \theta_1 \\ \chi_1 \end{Bmatrix} = \begin{Bmatrix} 1 \\ -1 \end{Bmatrix} \tag{3.40}$$

The energy coefficient

$$A_3 = P_3(u_1) = 0 \tag{3.41}$$

Eq. (2.33) for this example gives

$$\{(KI^2 - 2\lambda I)\theta_2 + \lambda I\chi_2 + \frac{3}{2}K\frac{I^3}{I_s}\theta_1^2\}\,\delta\theta + \{\lambda I\theta_2 + (KI^2 - 2\lambda I)\chi_2 + \frac{3}{2}K\frac{I^3}{I_s}\chi_1^2\}\,\delta\chi = 0 \tag{3.42}$$

From Eqs. (3.39), (3.40) and since $\delta\theta$, $\delta\chi$ are arbitrary, we get

$$\theta_2 + \chi_2 = -\frac{9}{2}\frac{I}{I_s} \tag{3.43}$$

Assuming

$$T_2(u) = \frac{1}{2}(\theta^2 + \chi^2) \tag{3.44}$$

then Eq. (2.34) gives

$$\theta_1\theta_2 + \chi_1\chi_2 = 0 \tag{3.45}$$

Using Eq. (3.40) the above equation becomes

$$\theta_2 = \chi_2 \tag{3.46}$$

Hence, from Eqs. (3.43) and (3.46)

$$\theta_2 = \chi_2 = -\frac{9}{4}\frac{l}{l_s} \tag{3.47}$$

The energy coefficients A_4 and A_2' are given by (from Eqs. (2.26), (2.30), (3.32), (3.34), (3.40), (3.47))

$$A_4 = -\left(\frac{3}{2} + \frac{25}{4}\frac{l^2}{l_s^2}\right) \tag{3.48}$$

$$A_2' = -3l \tag{3.49}$$

The postbuckling coefficients are (from Eqs. (2.42), (2.43), (3.41), (3.48), (3.49))

$$\hat{a} = 0 \tag{3.50}$$

$$\hat{b} = -\left(\frac{3}{2} + \frac{25}{4}\frac{l^2}{l_s^2}\right) \tag{3.51}$$

3.2.2 Engineering Strain

The Engineering strain in the springs is

$$\varepsilon_1 = \frac{\delta_1}{l_s} \tag{3.52}$$

$$\varepsilon_2 = \frac{\delta_2}{l_s} \tag{3.53}$$

From Eqs. (3.18) to (3.22), (3.52), (3.53); neglecting fourth and higher order terms, the nonlinear equilibrium equations are

$$KI\left(\theta - \frac{2}{3}\theta^3\right) - \lambda\left(2\theta - \chi - \frac{1}{3}\theta^3 - \theta^2\chi + \frac{3}{2}\theta\chi^2 - \frac{1}{3}\chi^3\right) = 0 \tag{3.54}$$

$$KI\left(\chi - \frac{2}{3}\chi^3\right) - \lambda\left(-\theta + 2\chi - \frac{1}{3}\theta^3 + \frac{3}{2}\theta^2\chi - \theta\chi^2 - \frac{1}{3}\chi^3\right) = 0 \tag{3.55}$$

Linearizing the equilibrium Eqs. (3.54), (3.55)

$$(KI - 2\lambda)\theta + \lambda\chi = 0 \tag{3.56}$$

$$\lambda\theta + (KI - 2\lambda)\chi = 0 \tag{3.57}$$

These are the same as for Green's strain measure.

The potential energy P(u) of transition from the fundamental state to an adjacent state is given by Eq. (3.9), where

$$P_1(u) = \Pi_1(u) = 0 \tag{3.58}$$

$$P_2(u) = \Pi_2(u) = \frac{1}{2} KI^2(\theta^2 + \chi^2) - \lambda I(\theta^2 + \chi^2 - \theta\chi) \tag{3.59}$$

$$P_3(u) = \Pi_3(u) = 0 \tag{3.60}$$

$$P_4(u) = \Pi_4(u) = -\frac{1}{6} KI^2(\theta^4 + \chi^4)$$

$$+ \frac{\lambda I}{12}(\theta^4 + 4\theta^3\chi - 9\theta^2\chi^2 + 4\theta\chi^3 + \chi^4) \tag{3.61}$$

Following the same procedure as for Green's strain, we get the energy and postbuckling coefficients as

$$A_3 = 0 \tag{3.62}$$

$$A_4 = -\frac{3}{2} \tag{3.63}$$

$$A_2' = -3I \tag{3.64}$$

$$\hat{a} = 0 \tag{3.65}$$

$$\hat{b} = -\frac{3}{2} \tag{3.66}$$

Comparing Eqs. (3.51) and (3.66) we see that the postbuckling coefficient $\hat{b}$ can be very different for small values of l_s. However, for small values of l_s, the small strain region ($\varepsilon \leq 0.01$) is very limited. This is evident in the load displacement plot shown in Fig. 5. For $l_s = 1$ the two strain measures result in widely different curves. However, the small strain region is $a < 0.01$ and the two curves don't manage to diverge much in

that region. For $l_s = 10$ the small strain region is large, $a \leq 0.1001$, but the two curves are almost identical.

The difference in the load-displacement behavior for Engineering strain and Green's strain may have been exaggerated by assuming that the stress strain relation for both cases follows Hooke's law (is linear). With the same Young's modulus, obviously if one follows that law the other has a nonlinear stress-strain relationship.

In case of truss elements the strain corresponding to the first order Piola-Kirchhoff stress is same as the engineering strain. The type of stress measure used by EAL for other elements is not known.

Chapter 4 : Koiter's Method in Finite Element Form

The matrix procedure based upon finite element idealization is taken from the work of Haftka, Mallett and Nachbar [3,4]. The notation followed is that of Mallett and Marcal [27].

The finite element representation of a geometrically nonlinear structure is taken as,

$$\Pi(Q) = \{Q\}^T[\frac{1}{2}[K] + \frac{1}{6}[N_1(Q)] + \frac{1}{12}[N_2(Q)]]\{Q\} - \{Q\}^T\{P\} \qquad (4.1)$$

where

$\Pi(Q)$	is the total potential energy
Q	is a displacement degree of freedom
{Q}	is the set of displacement degrees of freedom
{P}	is the applied load vector
[K]	is the linear stiffness matrix
$[N_1(Q)]$	is the first order incremental stiffness matrix
$[N_2(Q)]$	is the second order incremental stiffness matrix

The analysis begins from the energy functional of Eq. (2.2),

$$\Pi(U) = \Pi_1(U) + \Pi_2(U) + \Pi_3(U) + \Pi_4(U) + \ldots \tag{4.2}$$

for which the discretized finite element form can be written as

$$\Pi(Q) = \Pi_1(Q) + \Pi_2(Q) + \Pi_3(Q) + \Pi_4(Q) \tag{4.3}$$

where

$$\Pi_1(Q) = -\{Q\}^T\{P\} \tag{4.4}$$

$$\Pi_2(Q) = \frac{1}{2}\{Q\}^T[K]\{Q\} \tag{4.5}$$

$$\Pi_3(Q) = \frac{1}{6}\{Q\}^T[N_1(Q)]\{Q\} \tag{4.6}$$

$$\Pi_4(Q) = \frac{1}{12}\{Q\}^T[N_2(Q)]\{Q\} \tag{4.7}$$

The matrix equation governing determination of the fundamental path is found by setting the first variation of the potential energy equal to zero in accord with Eq. (2.5),

$$\delta\Pi(Q) = 0 = \Pi_1(\delta Q) + \Pi_{11}(\delta Q,Q) + \Pi_{12}(\delta Q,Q) + \Pi_{13}(\delta Q,Q) \tag{4.8}$$

or

$$\delta\Pi(Q) = 0 = \{\delta Q\}^T[\,[K] + \frac{1}{2}[N_1(Q)] + \frac{1}{3}[N_2(Q)]\,]\{Q\} - \{\delta Q\}^T\{P\} \tag{4.9}$$

Koiter's method presumes knowledge of the solution to Eq. (4.9) as $\{Q\} = \{Q(\lambda)\}$. Because Eq. (4.9) is nonlinear, such solutions are generally difficult to obtain. For a sig-

nificant number of problems, although Eq. (4.9) is nonlinear, the actual fundamental path is linear or approximately linear, and may be calculated from the linearized form of Eq. (4.9)

$$\delta\Pi(Q) = 0 = \{\delta Q\}^T[K]\{Q\} - \{\delta Q\}^T\{P\} \tag{4.10}$$

from which the linearized displacement $\{Q(\lambda)\}$ corresponding to Eq. (2.7) is obtained as

$$\{Q(\lambda)\} = \lambda\{Q_0\} = [K]^{-1}\lambda\{P_0\} \tag{4.11}$$

For a small displacement variation {q} from the fundamental equilibrium state to an adjacent state, the transition energy functional corresponding to Eq. (2.9) is given by

$$P(q) = P_2(q) + P_3(q) + P_4(q) \tag{4.12}$$

where

$$P_2(q) = \Pi_2(q) + \Pi_{21}(q,Q) + \Pi_{22}(q,Q)$$

$$= \frac{1}{2}\{q\}^T[\,[K] + \lambda\,[N_1(Q_0)] + \lambda^2\,[N_2(Q_0)]\,]\{q\} \tag{4.13}$$

$$P_3(q) = \Pi_3(q) + \Pi_{31}(q,Q)$$

$$= \frac{1}{6}\{q\}^T[\,[N_1(q)] + \lambda\,[N_{11}(q,Q_0)]\,]\{q\} \tag{4.14}$$

$$P_4(q) = \Pi_4(q)$$

$$= \frac{1}{12}\{q\}^T[N_2(q)]\{q\} \tag{4.15}$$

From Eq. (4.13) and the relation of Eq. (2.18) the equation governing determination of the bifurcation point is

$$P_{11}(\delta q,q) = 0 = \{\delta q\}^T[\,[K] + \lambda\,[N_1(Q_0)] + \lambda^2\,[N_2(Q_0)]\,]\{q\} \tag{4.16}$$

The quadratic eigenvalue problem resulting from Eq. (4.16) for arbitrary $\{\delta q\}$ is assumed to give a smallest possible eigenvalue λ_1 and a unique eigenvector $\{q\} = \{q_1\}$.

The finite element procedure of Koiter's method for predicting the initial post-buckling behavior is essentially complete upon specification of the coefficients in the single degree of freedom potential energy given as Eq. (2.25).

Assuming the arbitrary positive definite quadratic functional $T_2(q)$ as

$$T_2(q) = \frac{1}{2}\{q\}^T\{q\} \tag{4.17}$$

Eqs. (2.31), (2.32) for $\{\phi_1'\}$ now become

$$[K_T]\{\phi_1'\} = \{r_1\} \quad ; \qquad \{q_1\}^T\{\phi_1'\} = 0 \tag{4.18}$$

where $[K_T]$ is the tangential stiffness matrix.

$$[K_T] = [K] + \lambda_1\,[N_1(Q_0)] + \lambda_1{}^2\,[N_2(Q_0)] \tag{4.19}$$

and

$$\{r_1\} = \frac{\{q_1\}^T[\,[N_1(Q_0)] + 2\lambda_1\,[N_2(Q_0)]\,]\{q_1\}}{\{q_1\}^T\{q_1\}}\{q_1\}$$

$$- [\,[N_1(Q_0)] + 2\lambda_1\,[N_2(Q_0)]\,]\{q_1\} \tag{4.20}$$

Eqs. (2.33), (2.34) for $\{\phi_2\}$ now become

$$[K_T]\{\phi_2\} = \{r_2\} \quad ; \qquad \{q_1\}^T\{\phi_2\} = 0 \tag{4.21}$$

where,

$$\{r_2\} = \frac{\frac{1}{2}\{q_1\}^T[\,[N_1(q_1)] + \lambda_1\,[N_{11}(q_1, Q_0)]\,]\{q_1\}}{\{q_1\}^T\{q_1\}}\{q_1\}$$

$$-\frac{1}{2}[\,[N_1(q_1)] + \lambda_1\,[N_{11}(q_1, Q_0)]\,]\{q_1\} \tag{4.22}$$

The coefficients A_2', A_2'', etc., are given by Eqs. (2.26) to (2.30), expressed in finite element notation:

$$A_2' = -\frac{1}{2\lambda_1}\{q_1\}^T[\,2[K] + \lambda_1\,[N_1(Q_0)]\,]\{q_1\} \tag{4.23}$$

$$A_2'' = \frac{1}{2}\{q_1\}^T[N_2(Q_0)]\{q_1\} - \frac{1}{2}\{\phi_1'\}^T[K_T]\{\phi_1'\} \tag{4.24}$$

$$A_3 = \frac{1}{6}\{q_1\}^T[\,[N_1(q_1)] + \lambda_1\,[N_{11}(Q_0, q_1)]\,]\{q_1\} \tag{4.25}$$

$$A_3' = \frac{1}{6}\{q_1\}^T[N_{11}(Q_0, q_1)]\{q_1\} - \{\phi_1'\}^T[K_T]\{\phi_2\} \tag{4.26}$$

$$A_4 = \frac{1}{12}\{q_1\}^T[N_2(q_1)]\{q_1\} - \frac{1}{2}\{\phi_2\}^T[K_T]\{\phi_2\} \tag{4.27}$$

Chapter 5 : Stiffness Matrices

5.1 *Displacement Formulation*

The total potential in finite element form is given by Eq. (4.1). Differentiating this equation gives the equilibrium equation

$$[\,[K] + \frac{1}{2}[N_1(Q)] + \frac{1}{3}[N_2(Q)]\,]\{Q\} - \{P\} = \{0\} \tag{5.1}$$

Differentiating this equilibrium equation gives the linear incremental equilibrium equation

$$[\,[K] + [N_1(Q)] + [N_2(Q)]\,]\{\Delta Q\} - \{\Delta P\} = \{0\} \tag{5.2}$$

For the Eqs. (4.1), (5.1), and (5.2) the notation used is that of Mallett and Marcal [27]. In general, Eqs. (5.1) and (5.2) do not necessarily follow from (4.1). The difficulty with the notation is due to the fact that the expressions used to evaluate the incremental

stiffness matrices $[N_1]$ and $[N_2]$ in Eq. (4.1) are not unique. However, there are particular forms of expressions for these matrices for which the formalism of Eqs. (4.1), (5.1), (5.2) is always valid, and general expressions for which this is true were derived by Rajasekharan and Murray [28]. The procedure is briefly described here.

The total potential for a linear elastic element can be written as

$$\Pi = \frac{1}{2} \int_V \varepsilon_i C_{ij} \varepsilon_j \, dV - \{Q\}^T \{P\} \tag{5.3}$$

where

$\varepsilon_i, \varepsilon_j$	are components of Green's strain tensor
C_{ij}	are linear elastic constitutive coefficients
V	is volume of the element
dV	is an infinitesimal volume of the element

and the repeated indices are summed from 1 to 6.

Each strain component can be decomposed into two parts and written as

$$\varepsilon_i = \varepsilon_i^l + \varepsilon_i^{nl} \tag{5.4}$$

in which ε_i^l is linearly dependent on displacements and ε_i^{nl} is quadratically dependent on displacements.

From relations (5.3) and (5.4)

$$\Pi = \frac{1}{2} \int_V C_{ij} (\varepsilon_i^l \varepsilon_j^l + 2\varepsilon_i^l \varepsilon_j^{nl} + \varepsilon_i^{nl} \varepsilon_j^{nl}) \, dV - \{Q\}^T \{P\} \tag{5.5}$$

Equation (5.4) may be written as

$$\varepsilon_i = \{L_i\}^T\{d\} + \frac{1}{2}\{d\}^T[H_i]\{d\} \tag{5.6}$$

where

$\{L_i\}$	is a vector
$[H_i]$	is a symmetric matrix
{d}	is the vector of displacement gradients

For example, consider the truss element of Fig. 6. Let u, v, w be the displacements in the x, y, and z coordinate directions respectively and a comma denote partial differentiation with respect to the following coordinate. For this element there is only one strain component that contributes to the strain energy. Hence the range of i in Eq. (5.6) is one and the subscript can be dropped. For this element, Eq. (5.6) is

$$\varepsilon = u_{,x} + \frac{1}{2}\{(u_{,x})^2 + (v_{,x})^2 + (w_{,x})^2\} \tag{5.7}$$

from which

$$\{d\}^T = \{\, u_{,x} \;\; v_{,x} \;\; w_{,x} \,\} \tag{5.8}$$

$$\{L\}^T = \{\, 1 \;\; 0 \;\; 0 \,\} \tag{5.9}$$

$$[H] = \begin{bmatrix} 1 & 0 & 0 \\ 0 & 1 & 0 \\ 0 & 0 & 1 \end{bmatrix} \tag{5.10}$$

and

$$\varepsilon = \{L\}^T\{d\} + \frac{1}{2}\{d\}^T[H]\{d\} \tag{5.11}$$

Equation (5.6), in its more general form, represents each strain component by expressions of the type contained in Eqs. (5.7) to (5.11).

From Eqs. (5.5) and (5.6) the total potential,

$$\Pi = \frac{1}{2}\int_V C_{ij}\{d\}^T\left[\,[L_i][L_j]^T + [L_i]\{d\}^T[H_j] + \frac{1}{4}[H_i]\{d\}\{d\}^T[H_j]\,\right]\{d\}\,dV$$

$$- \{Q\}^T\{P\} \tag{5.12}$$

In the finite element model we express displacements in terms of nodal, or generalized coordinates.

$$\begin{Bmatrix} u \\ v \\ w \end{Bmatrix} = [N]\{Q\} \tag{5.13}$$

where [N] is the displacement function matrix.

Differentiating Eq. (5.13) to obtain displacement gradients

$$\{d\} = [D]\{Q\} \tag{5.14}$$

Writing Eq. (5.12) in the symbolic form

$$\Pi = \int_v \{d\}^T \left[\frac{1}{2} [\hat{K}] + \frac{1}{6} [\hat{N_1}] + \frac{1}{12} [\hat{N_2}] \right] \{d\} dV - \{Q\}^T \{P\} \tag{5.15}$$

where, in order that Eqs. (4.1), (5.1), and (5.2) apply

$$[\hat{K}] = C_{ij} \{L_i\} \{L_j\}^T \tag{5.16}$$

$$[\hat{N_1}] = C_{ij} \left(\{L_i\} \{d\}^T [H_j] + \{d\}^T \{L_i\} [H_j] + [H_i] \{d\} \{L_j\}^T \right) \tag{5.17}$$

$$[\hat{N_2}] = C_{ij} \left([H_i] \{d\} \{d\}^T [H_j] + \frac{1}{2} \{d\}^T [H_j] \{d\} [H_i] \right) \tag{5.18}$$

Comparing Eqs. (4.1) and (5.15) and using Eq. (5.14), the stiffness matrices are given by

$$[K] = \int_v [D]^T [\hat{K}] [D] \, dV \tag{5.19}$$

$$[N_1] = \int_v [D]^T [\hat{N_1}] [D] \, dV \tag{5.20}$$

$$[N_2] = \int_v [D]^T [\hat{N_2}] [D] \, dV \tag{5.21}$$

5.2 *Truss Element*

Consider the truss element shown in Fig. 6. The relevant displacement assumptions and matrices associated with that element are as follows.

The strain description is

$$\varepsilon = u_{,x} + \frac{1}{2}\{(u_{,x})^2 + (v_{,x})^2 + (w_{,x})^2\}$$

$$= \{L\}^T\{d\} + \frac{1}{2}\{d\}^T[H]\{d\} \tag{5.22}$$

from which

$$\{d\}^T = \{\, u_{,x} \;\; v_{,x} \;\; w_{,x} \,\} \tag{5.23}$$

$$\{L\}^T = \{\, 1 \;\; 0 \;\; 0 \,\} \tag{5.24}$$

$$[H] = \begin{bmatrix} 1 & 0 & 0 \\ 0 & 1 & 0 \\ 0 & 0 & 1 \end{bmatrix} \tag{5.25}$$

The displacement description is

$$\begin{Bmatrix} u \\ v \\ w \end{Bmatrix} = [N]\{Q\}$$

$$= \begin{bmatrix} 1-\zeta & 0 & 0 & \zeta & 0 & 0 \\ 0 & 1-\zeta & 0 & 0 & \zeta & 0 \\ 0 & 0 & 1-\zeta & 0 & 0 & \zeta \end{bmatrix} \{Q\} \tag{5.26}$$

where,

$$\zeta = \frac{x}{l} \tag{5.27}$$

$$\{Q\}^T = \{ u_1 \;\; v_1 \;\; w_1 \;\; u_2 \;\; v_2 \;\; w_2 \} \tag{5.28}$$

Differentiating Eq. (5.26) to obtain the displacement gradients

$$\begin{Bmatrix} u_{,x} \\ v_{,x} \\ w_{,x} \end{Bmatrix} = \frac{1}{l} \begin{bmatrix} -1 & 0 & 0 & 1 & 0 & 0 \\ 0 & -1 & 0 & 0 & 1 & 0 \\ 0 & 0 & -1 & 0 & 0 & 1 \end{bmatrix} \{Q\} \tag{5.29}$$

which defines the matrix [D] of Eq. (5.14)

Using Eqs. (5.16), (5.17), (5.18) gives

$$[\hat{K}] = E \begin{bmatrix} 1 & 0 & 0 \\ 0 & 0 & 0 \\ 0 & 0 & 0 \end{bmatrix} \tag{5.30}$$

$$[\hat{N}_1] = E \begin{bmatrix} 3u_{,x} & v_{,x} & w_{,x} \\ v_{,x} & u_{,x} & 0 \\ w_{,x} & 0 & u_{,x} \end{bmatrix} \tag{5.31}$$

$$[\hat{N}_2] = E \begin{bmatrix} \Delta + (u_{,x})^2 & u_{,x}v_{,x} & u_{,x}w_{,x} \\ u_{,x}v_{,x} & \Delta + (v_{,x})^2 & v_{,x}w_{,x} \\ u_{,x}w_{,x} & v_{,x}w_{,x} & \Delta + (w_{,x})^2 \end{bmatrix} \tag{5.32}$$

where

$$\Delta = \frac{1}{2}\{(u_{,x})^2 + (v_{,x})^2 + (w_{,x})^2\} \tag{5.33}$$

For the truss bar element having a cross-sectional area A and infinitesimal length dx in x direction, the infinitesimal volume,

$$dV = Adx \tag{5.34}$$

The displacement gradients and the matrices $[D]$, $[\hat{K}]$, $[\hat{N}_1]$, $[\hat{N}_2]$ are independent of the x coordinate (see Eqs. (5.29), (5.30), (5.31), (5.32)). Hence the integrands corresponding to Eqs. (5.19), (5.20), and (5.21) for a bar element of constant cross-sectional area can be taken out of the integral and the stiffness matrices written as

$$[K] = A \int [D]^T [\hat{K}][D] \tag{5.35}$$

$$[N_1] = A\,l\,[D]^T[\hat{N_1}][D] \tag{5.36}$$

$$[N_2] = A\,l\,[D]^T[\hat{N_2}][D] \tag{5.37}$$

Hence for a single truss element, using Eqs. (5.29), (5.30), (5.31), (5.32), (5.35), (5.36), and (5.37) the stiffness matrices are given by

$$[K] = \frac{EA}{l}\begin{bmatrix} 1 & 0 & 0 & -1 & 0 & 0 \\ 0 & 0 & 0 & 0 & 0 & 0 \\ 0 & 0 & 0 & 0 & 0 & 0 \\ -1 & 0 & 0 & 1 & 0 & 0 \\ 0 & 0 & 0 & 0 & 0 & 0 \\ 0 & 0 & 0 & 0 & 0 & 0 \end{bmatrix} \tag{5.38}$$

$$[N_1] = \frac{EA}{l}\begin{bmatrix} 3u_{,x} & v_{,x} & w_{,x} & -3u_{,x} & -v_{,x} & -w_{,x} \\ v_{,x} & u_{,x} & 0 & -v_{,x} & -u_{,x} & 0 \\ w_{,x} & 0 & u_{,x} & -w_{,x} & 0 & -u_{,x} \\ -3u_{,x} & -v_{,x} & -w_{,x} & 3u_{,x} & v_{,x} & w_{,x} \\ -v_{,x} & -u_{,x} & 0 & v_{,x} & u_{,x} & 0 \\ -w_{,x} & 0 & -u_{,x} & w_{,x} & 0 & u_{,x} \end{bmatrix} \tag{5.39}$$

$$[N_2] = \frac{EA}{l}\begin{bmatrix} \Delta+(u_{,x})^2 & u_{,x}v_{,x} & u_{,x}w_{,x} & -(\Delta+(u_{,x})^2) & -u_{,x}v_{,x} & -u_{,x}w_{,x} \\ u_{,x}v_{,x} & \Delta+(v_{,x})^2 & v_{,x}w_{,x} & -u_{,x}v_{,x} & -(\Delta+(v_{,x})^2) & -v_{,x}w_{,x} \\ u_{,x}w_{,x} & v_{,x}w_{,x} & \Delta+(w_{,x})^2 & -u_{,x}w_{,x} & -v_{,x}w_{,x} & -(\Delta+(w_{,x})^2) \\ -(\Delta+(u_{,x})^2) & -u_{,x}v_{,x} & -u_{,x}w_{,x} & \Delta+(u_{,x})^2 & u_{,x}v_{,x} & u_{,x}w_{,x} \\ -u_{,x}v_{,x} & -(\Delta+(v_{,x})^2) & -v_{,x}w_{,x} & u_{,x}v_{,x} & \Delta+(v_{,x})^2 & v_{,x}w_{,x} \\ -u_{,x}w_{,x} & -v_{,x}w_{,x} & -(\Delta+(w_{,x})^2) & u_{,x}w_{,x} & v_{,x}w_{,x} & \Delta+(w_{,x})^2 \end{bmatrix}$$

(5.40)

For a planar truss element (no displacements in z direction) the stiffness matrices are given by

$$[K] = \frac{EA}{l}\begin{bmatrix} 1 & 0 & -1 & 0 \\ 0 & 0 & 0 & 0 \\ -1 & 0 & 1 & 0 \\ 0 & 0 & 0 & 0 \end{bmatrix} \tag{5.41}$$

$$[N_1] = \frac{EA}{l}\begin{bmatrix} 3u_{,x} & v_{,x} & -3u_{,x} & -v_{,x} \\ v_{,x} & u_{,x} & -v_{,x} & -u_{,x} \\ -3u_{,x} & -v_{,x} & 3u_{,x} & v_{,x} \\ -v_{,x} & -u_{,x} & v_{,x} & u_{,x} \end{bmatrix} \tag{5.42}$$

$$[N_2] = \frac{EA}{l}\begin{bmatrix} \Delta+(u_{,x})^2 & u_{,x}v_{,x} & -(\Delta+(u_{,x})^2) & -u_{,x}v_{,x} \\ u_{,x}v_{,x} & \Delta+(v_{,x})^2 & -u_{,x}v_{,x} & -(\Delta+(v_{,x})^2) \\ -(\Delta+(u_{,x})^2) & -u_{,x}v_{,x} & \Delta+(u_{,x})^2 & u_{,x}v_{,x} \\ -u_{,x}v_{,x} & -(\Delta+(v_{,x})^2) & u_{,x}v_{,x} & \Delta+(v_{,x})^2 \end{bmatrix} \tag{5.43}$$

where

$$\Delta = \frac{1}{2}\{(u_{,x})^2 + (v_{,x})^2\} \tag{5.44}$$

The tangent stiffness is the sum of the linear and incremental stiffnesses.

$$[K_T] = \frac{EA}{l}\begin{bmatrix} 1+3u_{,x}+\frac{3}{2}u_{,x}^2+\frac{1}{2}v_{,x}^2 & v_{,x}+u_{,x}v_{,x} & -1-3u_{,x}-\frac{3}{2}u_{,x}^2-\frac{1}{2}v_{,x}^2 & -v_{,x}-u_{,x}v_{,x} \\ v_{,x}+u_{,x}v_{,x} & u_{,x}+\frac{1}{2}u_{,x}^2+\frac{3}{2}v_{,x}^2 & -v_{,x}-u_{,x}v_{,x} & -u_{,x}-\frac{1}{2}u_{,x}^2-\frac{3}{2}v_{,x}^2 \\ -1-3u_{,x}-\frac{3}{2}u_{,x}^2-\frac{1}{2}v_{,x}^2 & -v_{,x}-u_{,x}v_{,x} & 1+3u_{,x}+\frac{3}{2}u_{,x}^2+\frac{1}{2}v_{,x}^2 & v_{,x}+u_{,x}v_{,x} \\ -v_{,x}-u_{,x}v_{,x} & -u_{,x}-\frac{1}{2}u_{,x}^2-\frac{3}{2}v_{,x}^2 & v_{,x}+u_{,x}v_{,x} & u_{,x}+\frac{1}{2}u_{,x}^2+\frac{3}{2}v_{,x}^2 \end{bmatrix} \tag{5.45}$$

5.3 *Stiffness Matrices by EAL*

The stiffness matrices are obtained by using the geometric non-linear procedure of EAL320. The procedure follows the updated Lagrangian approach. It is briefly described here.

A local coordinate system is attached to each element. The local system moves with the element and therefore shares its rigid body motion. The current deformed state is used as the reference state prior to the next incremental step of the solution. Then the local coordinates are updated to produce a new reference state. The advantage of this corotational local system is that strains and rotations in the local system are usually small and higher order terms can be neglected. Essential nonlinearities are accounted

for by tracking the orientations of the several local systems. The resulting non-linear system of equilibrium equations can be solved by various algorithms.

EAL uses the modified Newton-Raphson method to solve the non-linear equations. It involves equations expressed in terms of displacement increments.

$$[K_T]\{\Delta Q\} + \{\Delta P\} = 0 \tag{5.46}$$

where

$[K_T]$	is the tangent stiffness matrix
$\{\Delta Q\}$	is incremental displacement vector
$\{\Delta P\}$	is incremental load vector

For a truss element the procedure adopted to obtain the tangent stiffness is as follows. Consider a truss element which undergoes some small displacements and rotation as shown in Fig. 7. The linear stiffness and the initial stress stiffness in the local corotational system of the element is

$$[K]_L = \frac{EA}{l}\begin{bmatrix} 1 & 0 & -1 & 0 \\ 0 & 0 & 0 & 0 \\ -1 & 0 & 1 & 0 \\ 0 & 0 & 0 & 0 \end{bmatrix} \tag{5.47}$$

$$[K_\sigma]_L = \frac{P}{l_f}\begin{bmatrix} 0 & 0 & 0 & 0 \\ 0 & 1 & 0 & -1 \\ 0 & 0 & 0 & 0 \\ 0 & -1 & 0 & 1 \end{bmatrix} \tag{5.48}$$

where

$$P = \frac{EA\ (l_f - l)}{l} \tag{5.49}$$

The tangent stiffness

$$[K_T]_L = [K]_L + [K_\sigma]_L \tag{5.50}$$

The ratio of initial to final length is

$$\frac{l}{l_f} = [(1 + u_{,x})^2 + v_{,x}{}^2]^{-1/2} \tag{5.51}$$

$$\simeq 1 - u_{,x} + u_{,x}{}^2 - \frac{v_{,x}{}^2}{2} + O_3(u_{,x}, v_{,x}) \tag{5.52}$$

If θ is the rotation, then the tangent stiffness in the original coordinate system is

$$[K_T] = [T]^T\ [K_T]_L\ [T] \tag{5.53}$$

where

$$[T] = \begin{bmatrix} \cos\theta & \sin\theta & 0 & 0 \\ -\sin\theta & \cos\theta & 0 & 0 \\ 0 & 0 & \cos\theta & \sin\theta \\ 0 & 0 & -\sin\theta & \cos\theta \end{bmatrix} \tag{5.54}$$

$$\cos\theta = \frac{l}{l_f}(1 + u_{,x}) \tag{5.55}$$

$$\sin\theta = \frac{l}{l_f} v_{,x} \tag{5.56}$$

Neglecting terms of order three and higher in $u_{,x}$, $v_{,x}$ and using Eqs. (5.47) to (5.56), the tangent stiffness is

$$[K_T] = \frac{EA}{l} \begin{bmatrix} 1-v_{,x}^2 & v_{,x}-2u_{,x}v_{,x} & -(1-v_{,x}^2) & -(v_{,x}-2u_{,x}v_{,x}) \\ v_{,x}-2u_{,x}v_{,x} & u_{,x}-u_{,x}^2+\frac{3}{2}v_{,x}^2 & -(v_{,x}-2u_{,x}v_{,x}) & -(u_{,x}-u_{,x}^2+\frac{3}{2}v_{,x}^2) \\ -(1-v_{,x}^2) & -(v_{,x}-2u_{,x}v_{,x}) & 1-v_{,x}^2 & v_{,x}-2u_{,x}v_{,x} \\ -(v_{,x}-2u_{,x}v_{,x}) & -(u_{,x}-u_{,x}^2+\frac{3}{2}v_{,x}^2) & v_{,x}-2u_{,x}v_{,x} & u_{,x}-u_{,x}^2+\frac{3}{2}v_{,x}^2 \end{bmatrix} \tag{5.57}$$

Denoting the difference in the stiffness matrices obtained by EAL to those from displacement formulation based on Green's strain, by a prefix Δ, the difference in tangent stiffness is (see Eqs. (5.45), (5.57)),

$$[\Delta K_T] = \frac{EA}{l} \begin{bmatrix} -3u_{,x}-\frac{3}{2}(u_{,x}^2+v_{,x}^2) & -3u_{,x}v_{,x} & 3u_{,x}+\frac{3}{2}(u_{,x}^2+v_{,x}^2) & 3u_{,x}v_{,x} \\ -3u_{,x}v_{,x} & -\frac{3}{2}u_{,x}^2 & 3u_{,x}v_{,x} & \frac{3}{2}u_{,x}^2 \\ 3u_{,x}+\frac{3}{2}(v_{,x}^2+u_{,x}^2) & 3u_{,x}v_{,x} & -3u_{,x}-\frac{3}{2}(u_{,x}^2+v_{,x}^2) & -3u_{,x}v_{,x} \\ 3u_{,x}v_{,x} & \frac{3}{2}u_{,x}^2 & -3u_{,x}v_{,x} & -\frac{3}{2}u_{,x}^2 \end{bmatrix} \tag{5.58}$$

The tangent stiffness being the sum of the linear stiffness and the incremental stiffnesses, it can be used to find $[N_1]$ and $[N_2]$. The procedure followed to obtain them by EAL is as follows. Let q be the displacement for which the incremental stiffnesses are needed. For displacement aq the tangent stiffness

$$[K_T(aq)] \equiv [K] + a[N_1(q)] + a^2[N_2(q)] \tag{5.59}$$

Hence

$$[N_1(q)] = \frac{\partial[K_T(aq)]}{\partial a}\Big|_{a=0} \tag{5.60}$$

$$[N_2(q)] = \frac{\partial^2[K_T(aq)]}{\partial a^2}\Big|_{a=0} \tag{5.61}$$

These partial derivatives are approximated by a second order central difference scheme.

$$[N_1(q)] = \frac{[K_T(-2aq)] - 8[K_T(-aq)] + 8[K_T(aq)] - [K_T(2aq)]}{12\,a} \tag{5.62}$$

$$[N_2(q)] = \frac{-[K_T(-2aq)] + 16[K_T(-aq)] - 30[K] + 16[K_T(aq)] - [K_T(2aq)]}{12\,a^2} \tag{5.63}$$

By using small values of a (so that higher order terms can be neglected), but not so small as to get large round-off errors, we can obtain these matrices from EAL. However, numerical experimentation revealed that the errors are minimized for $10^{-4} < aq_{max} < 10^{-2}$.

For a single bar element extensive numerical experimentation was-done to determine the stiffness matrices by EAL. They were found to be approximately given by

$$[K] = \frac{EA}{l}\begin{bmatrix} 1 & 0 & -1 & 0 \\ 0 & 0 & 0 & 0 \\ -1 & 0 & 1 & 0 \\ 0 & 0 & 0 & 0 \end{bmatrix} \tag{5.64}$$

$$[N_1] = \frac{EA}{l}\begin{bmatrix} 0 & v_{,x} & 0 & -v_{,x} \\ v_{,x} & u_{,x} & -v_{,x} & -u_{,x} \\ 0 & -v_{,x} & 0 & v_{,x} \\ -v_{,x} & -u_{,x} & v_{,x} & u_{,x} \end{bmatrix} \tag{5.65}$$

$$[N_2] = \frac{EA}{l}\begin{bmatrix} -(v_{,x})^2 & -2u_{,x}v_{,x} & (v_{,x})^2 & 2u_{,x}v_{,x} \\ -2u_{,x}v_{,x} & -(u_{,x})^2 + \frac{3}{2}(v_{,x})^2 & 2u_{,x}v_{,x} & (u_{,x})^2 - \frac{3}{2}(v_{,x})^2 \\ (v_{,x})^2 & 2u_{,x}v_{,x} & -(v_{,x})^2 & -2u_{,x}v_{,x} \\ 2u_{,x}v_{,x} & (u_{,x})^2 - \frac{3}{2}(v_{,x})^2 & -2u_{,x}v_{,x} & -(u_{,x})^2 + \frac{3}{2}(v_{,x})^2 \end{bmatrix} \tag{5.66}$$

These matrices (Eqs. (5.64), (5.65) and (5.66)) are the same as obtained by a Newton-Raphson procedure. The difference in the incremental stiffness matrices obtained by EAL to those from a displacement formulation based on Green's strain are (see Eqs. (5.42), (5.43), (5.65) and (5.66)),

$$[\Delta N_1] = \frac{EA}{l}\begin{bmatrix} -3u_{,x} & 0 & 3u_{,x} & 0 \\ 0 & 0 & 0 & 0 \\ 3u_{,x} & 0 & -3u_{,x} & 0 \\ 0 & 0 & 0 & 0 \end{bmatrix} \tag{5.67}$$

$$[\Delta N_2] = \frac{EA}{l}\begin{bmatrix} -\frac{3}{2}(v_{,x}^2 + u_{,x}^2) & -3u_{,x}v_{,x} & \frac{3}{2}(v_{,x}^2 + u_{,x}^2) & 3u_{,x}v_{,x} \\ -3u_{,x}v_{,x} & -\frac{3}{2}(u_{,x}^2) & 3u_{,x}v_{,x} & \frac{3}{2}(u_{,x}^2) \\ \frac{3}{2}(v_{,x}^2 + u_{,x}^2) & 3u_{,x}v_{,x} & -\frac{3}{2}(v_{,x}^2 + u_{,x}^2) & -3u_{,x}v_{,x} \\ 3u_{,x}v_{,x} & \frac{3}{2}(u_{,x}^2) & -3u_{,x}v_{,x} & -\frac{3}{2}(u_{,x}^2) \end{bmatrix} \quad (5.68)$$

The sum of $[\Delta N_1]$ and $[\Delta N_2]$gives $[\Delta K_T]$ (Eq. (5.58)). The incremental stiffnesses by EAL (Eqns. (5.65), (5.66)) are used to obtain A_3 (Eqn. (4.25)). Instead of obtaining A_2' using Eqn. (4.23), it can be directly obtained from the initial stress stiffness matrix. From Eqn. (4.13)

$$P_2(q) = \frac{1}{2}\{q\}^T[\,[K] + \lambda\,[N_1(Q_0)] + \lambda^2\,[N_2(Q_0)]\,]\{q\}$$

In terms of initial stress stiffness matrix, neglecting the initial displacement matrix

$$P_2(q) = \frac{1}{2}\{q\}^T[\,[K] + \lambda\,[K_\sigma(Q_0)]\,]\{q\} \quad (5.69)$$

Hence from Eqn. (2.26)

$$A_2' = P_2'(q_1)$$

$$= \frac{1}{2}\{q_1\}^T\,[K_\sigma(Q_0)]\,\{q_1\} \quad (5.70)$$

Chapter 6 : Examples

The examples presented here have been evaluated using a computer program based on the procedure stated earlier. Although only results for truss and beam structures have been presented, the program is general and is valid for any other structure because of the generality of the finite element method.

Lowest order energy approximations are used to get the post-buckling behavior. Hence for asymmetric bifurcating structures only the slope $\hat{a}$ is calculated. The behavior shown for the examples is a normalized load parameter λ with respect to the bifurcation load parameter λ_1 versus a selected displacement component.

6.1 Spring Bar Structure

The spring bar structure shown in Fig. 8 was solved analytically in section 3.1 for a case with rigid bars. When the bars are elastic, the structure has a non-linear pre-

buckling path. But since Koiter's method assumes a linear pre-buckling equilibrium path and is sensitive to pre-buckling nonlinearities, the pre-buckling displacements are not taken into account. The asymptotic analysis then yields the same slope as obtained analytically.

The behavior obtained is shown in Fig. 9. The structure exhibits an asymmetric bifurcation buckling. The equilibrium path obtained by solving the nonlinear equilibrium equations of the structure with small initial imperfections is also shown. It can be seen that the asymptotic procedure predicts the post-buckling behavior close to the bifurcation point.

6.2 *Knee Truss*

A knee truss consisting of 507 elements as shown in Fig. 10 also undergoes asymmetric bifurcation buckling. It also has a nonlinear pre-buckling equilibrium path and is not considered. The normalized load plotted versus the joint rotation at A is shown in Fig. 11. The equilibrium path obtained by solving the nonlinear equilibrium equations for the structure with the load placed eccentrically is also shown. The asymptotic analysis by the EAL procedure has given good asymptotic post-buckling behavior.

6.2 *Knee Frame*

The behavior of the knee frame structure with pinned supports as shown in Fig. 12, has been investigated experimentally by Roorda [19] and analytically by Koiter [13]. The measured and the results predicted by Koiter are in complete agreement.

If the load λ is applied directly above the column member the frame undergoes pre-buckling bending. But by placing the load λ at a uniquely determined neutral point such that there is negligible pre-buckling bending, the frame can be analysed by Koiter's method.

For the finite element analysis the frame is idealized as an assemblage of 40 elements of equal length. The asymptotic analysis by EAL predicts asymmetric bifurcation buckling and is shown in Fig. 13. It is compared to Roorda's experimental and Koiter's analytical results. The results obtained are in good agreement. The nonlinear load-displacement behavior for the frame with the load placed away from the neutral point is also shown in the figure. It shows that the procedure has predicted the post-buckling behavior asymptotically.

Chapter 7 : Conclusions

The first part of Koiter's method of analysis to predict post-buckling behavior close to the bifurcation point has been successfully implemented on finite element software EAL.

EAL is based on engineering strain measure. But it was shown that even though the post-buckling coefficients predicted for engineering strain are different from that predicted for Green's strain, the post-buckling behavior is approximately same. Since the computer procedure is based on Koiter's method of analysis, it has the same limitations as that of Koiter's method. Additional limitations of the procedure are that it is valid for problems with simple bifurcation points only (since multiple bifurcation structures are rare, they weren't considered) and external work contribution to the total potential energy is taken to be linearly dependent upon the displacement variable as is the customary practice in finite element analysis.

The automated computer procedure on EAL was used to obtain numerical results for truss and frame structures. They were compared to the nonlinear load-displacement

behavior for the structures with slight imperfections. Good agreement was observed. For the knee frame example the obtained post-buckling path was in agreement with available experimental and analytical results. Although the procedure was validated only for truss and frame structures, it should work for any other kind of structure because of the generality of the finite element method.

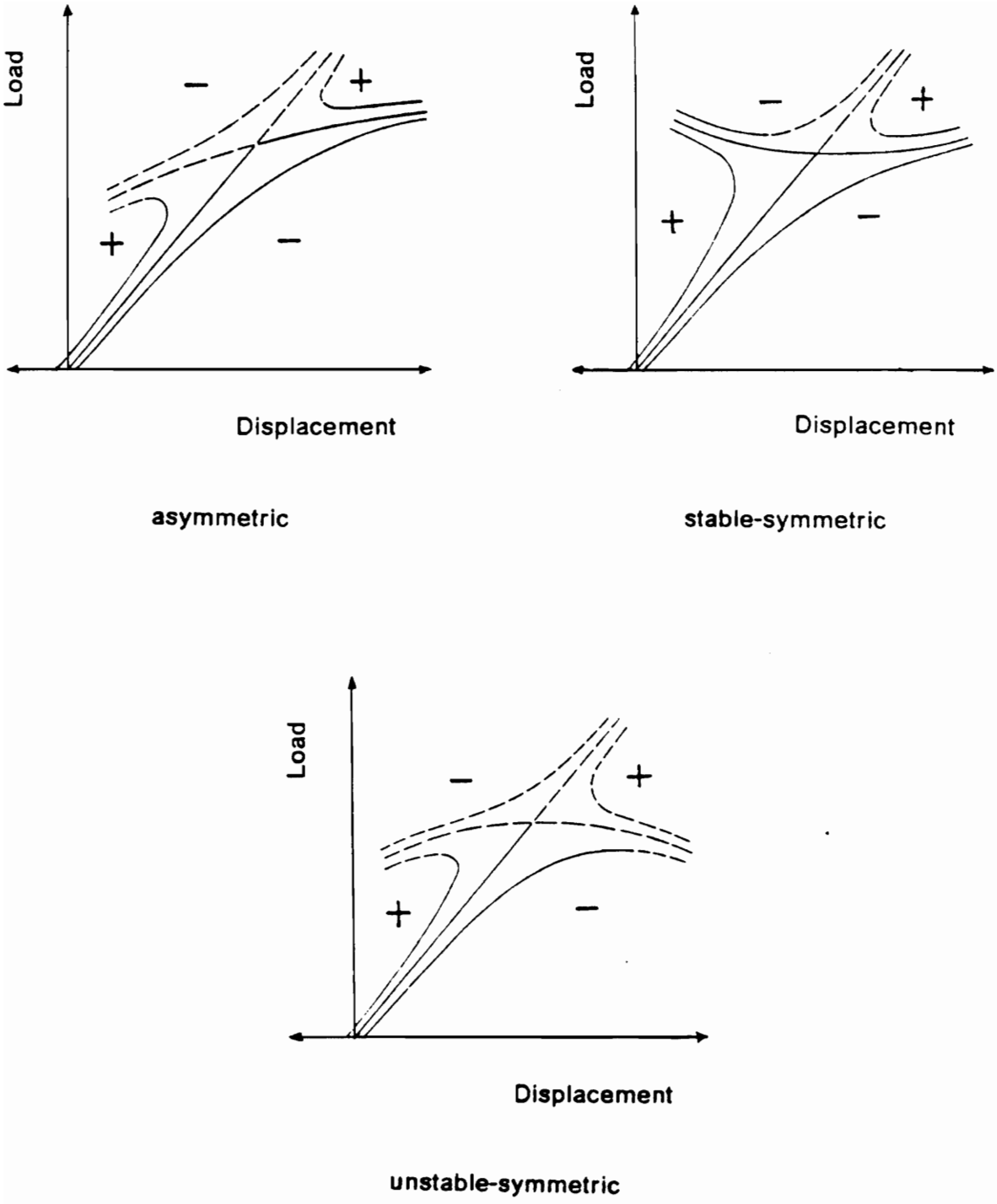

Figure 1. Types of bifurcation

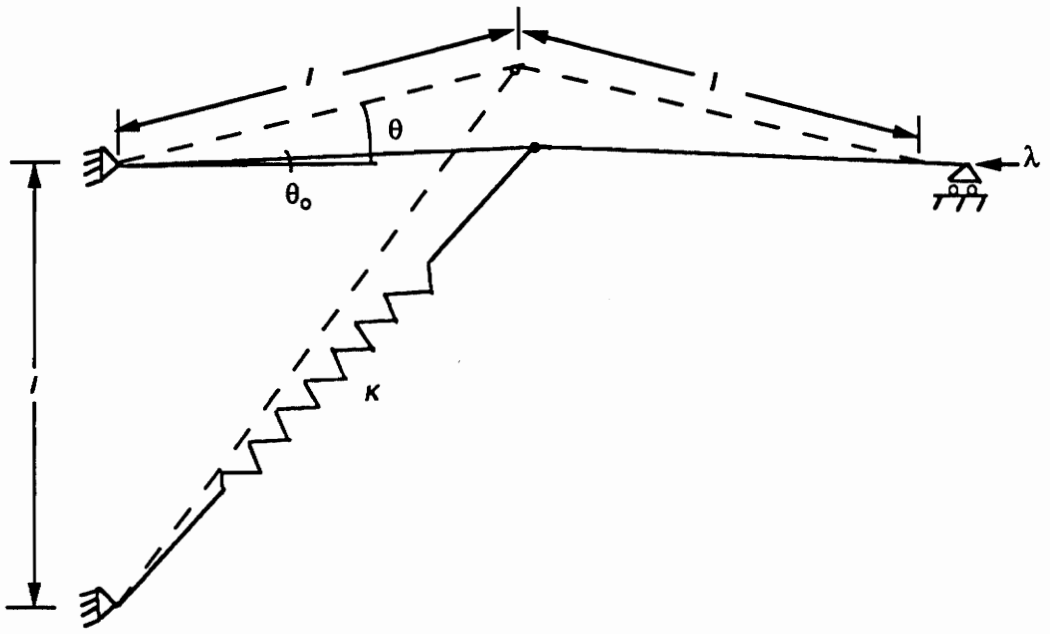

Figure 2. One degree of freedom model

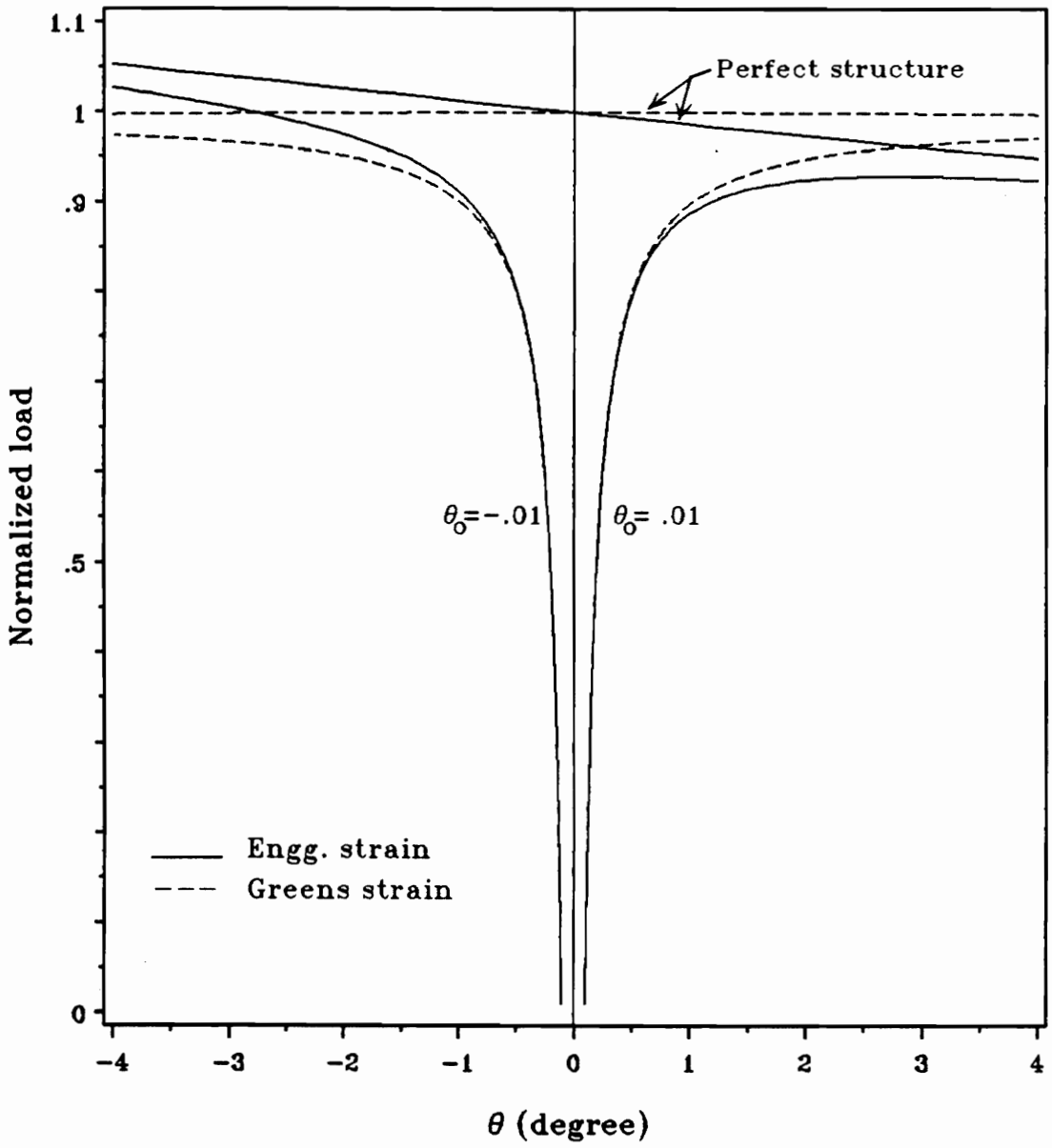

Figure 3. Load-displacement behavior for one degree of freedom model

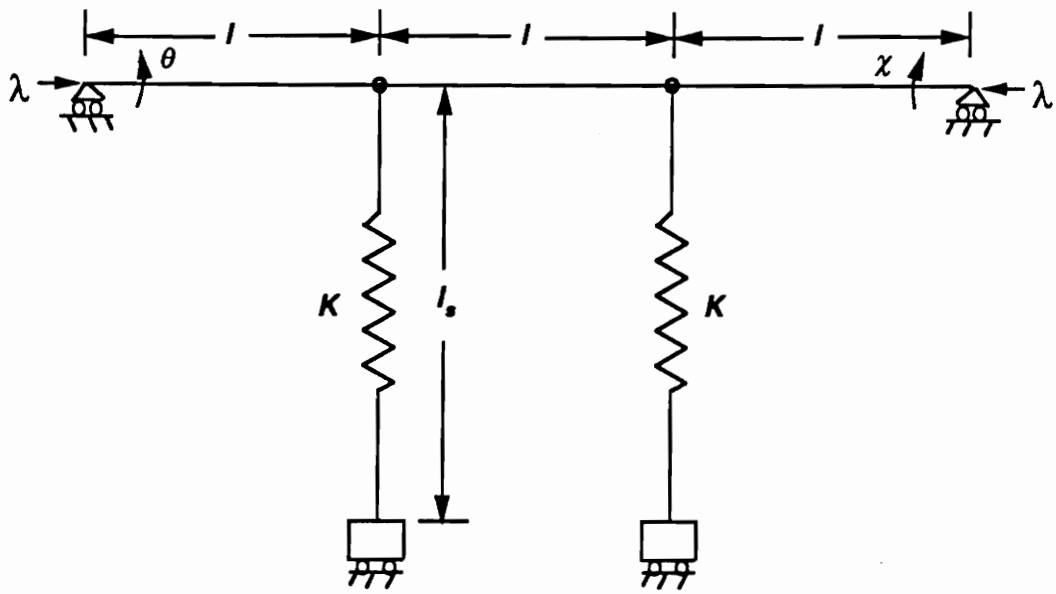

Figure 4. Two degrees of freedom model

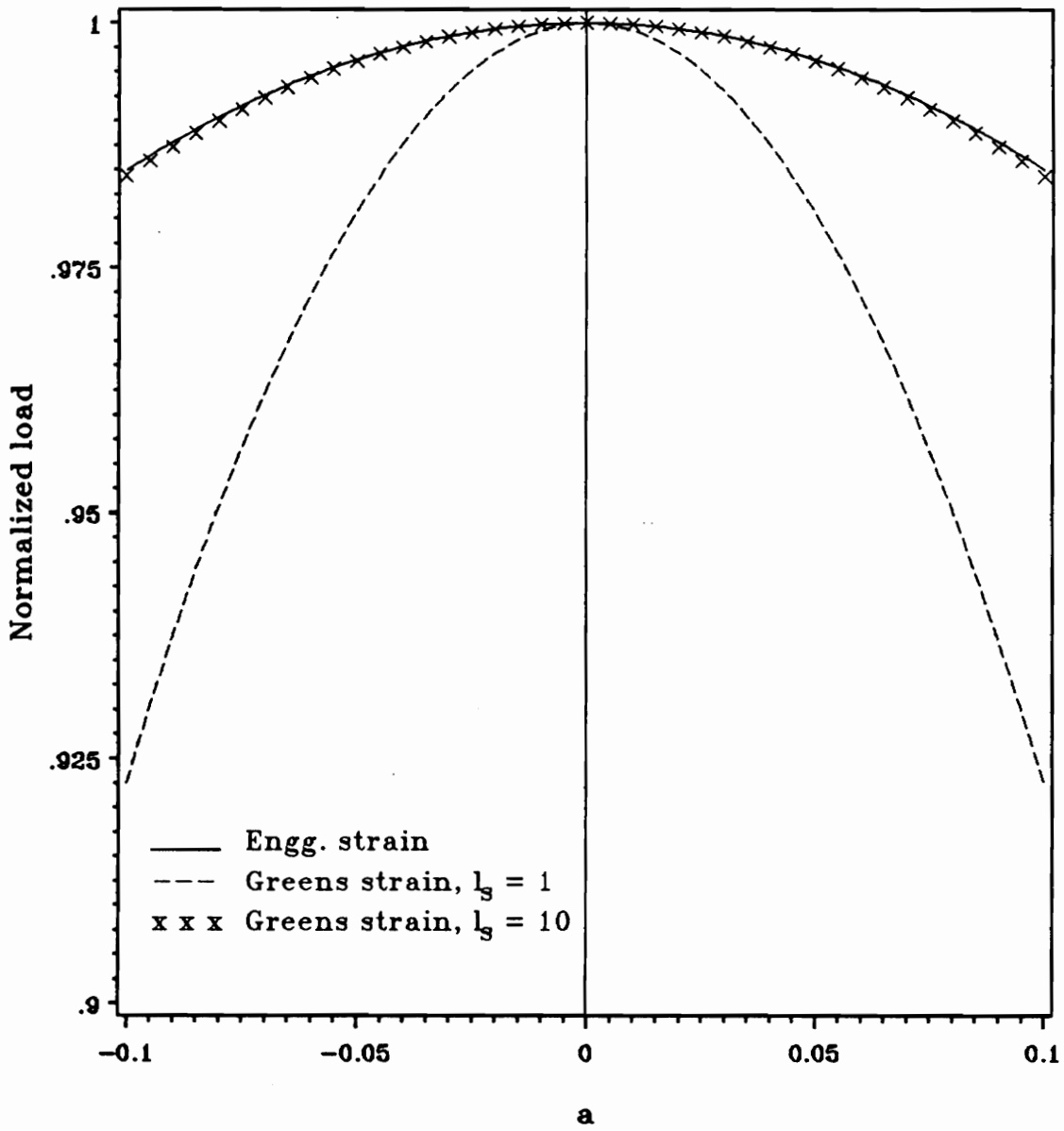

Figure 5. Load-displacement behavior for two degrees of freedom model

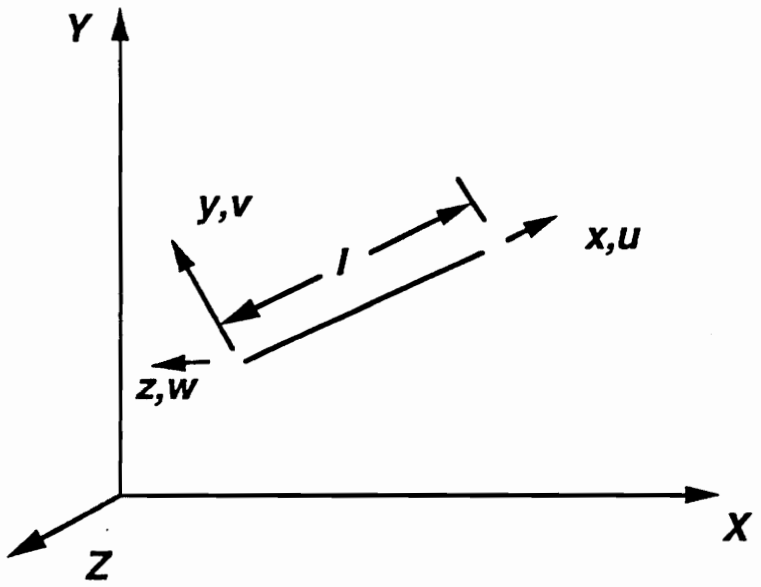

Figure 6. Truss element

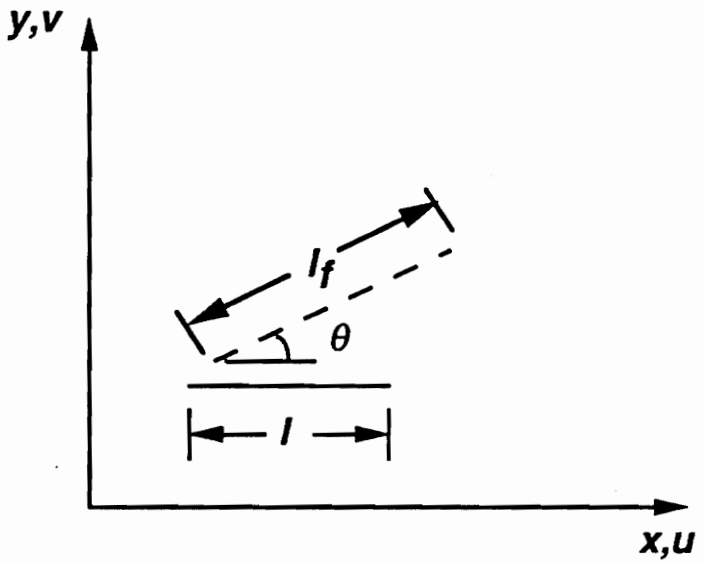

Figure 7. Truss element in X-Y plane

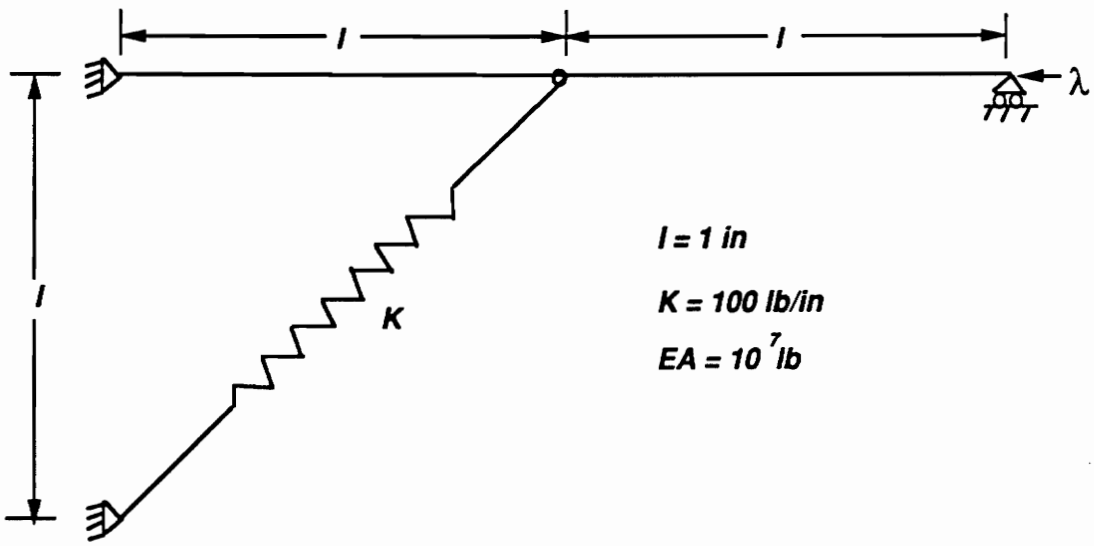

Figure 8. Spring bar structure

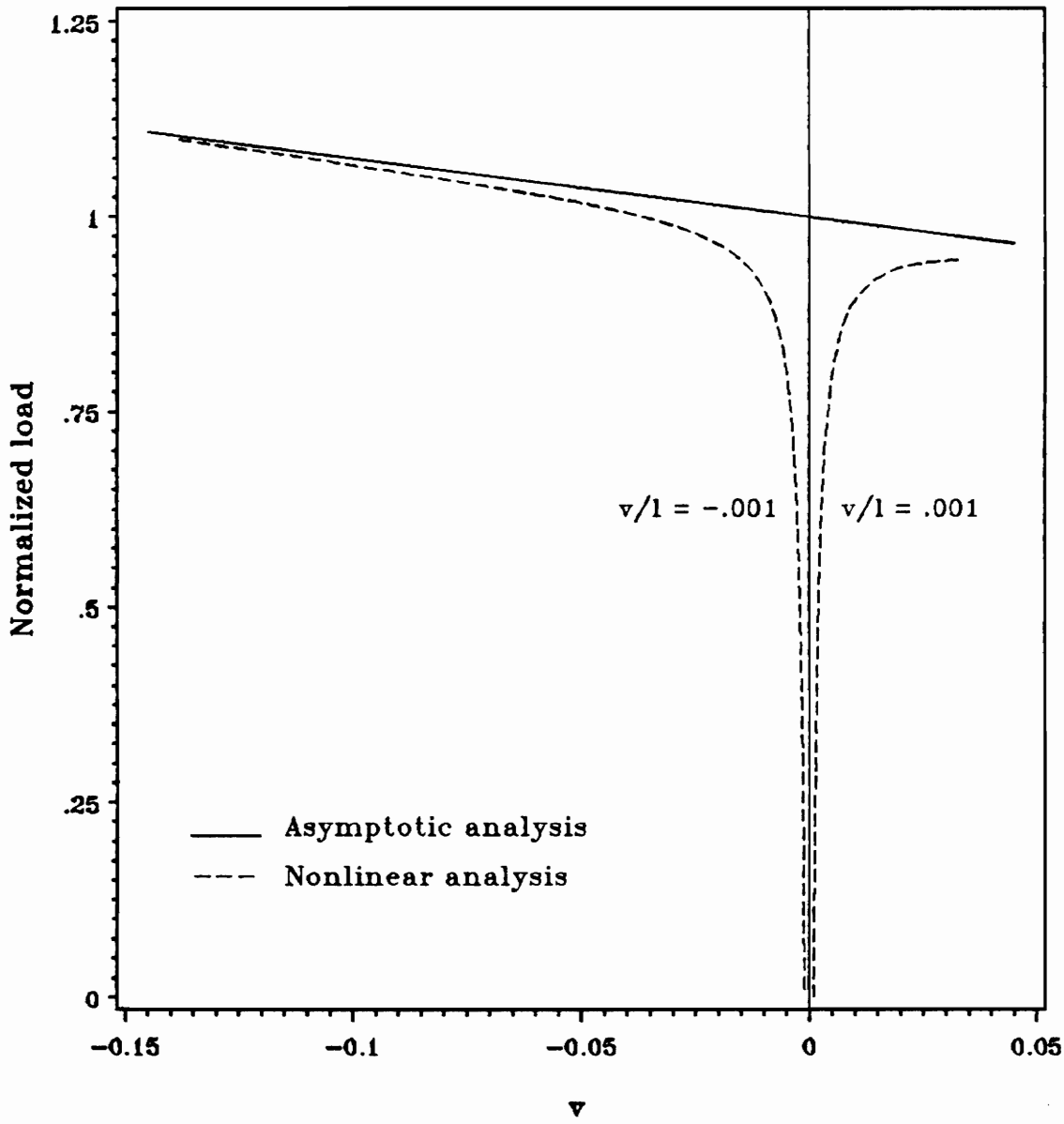

Figure 9. Load-displacement behavior for spring bar structure

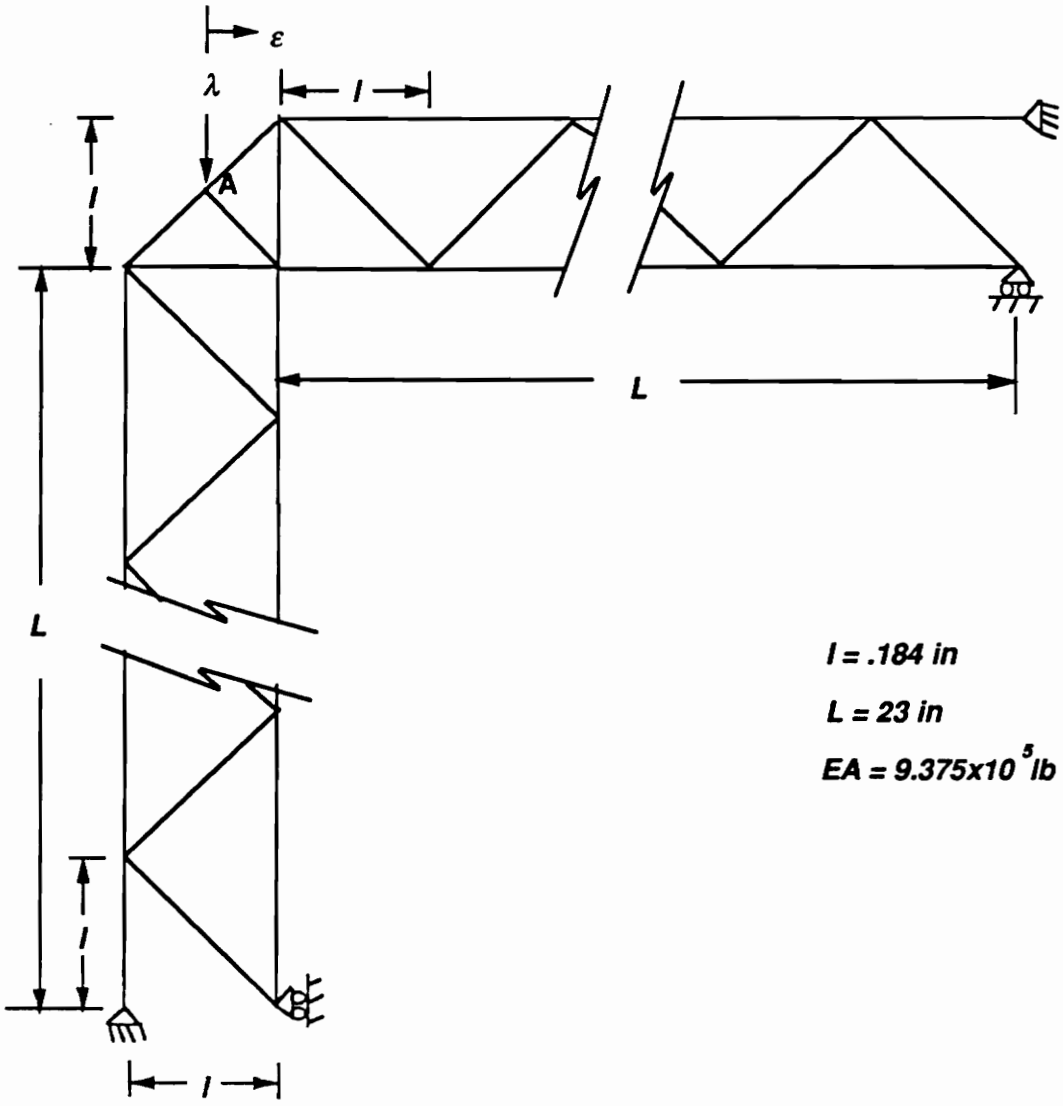

Figure 10. Knee truss

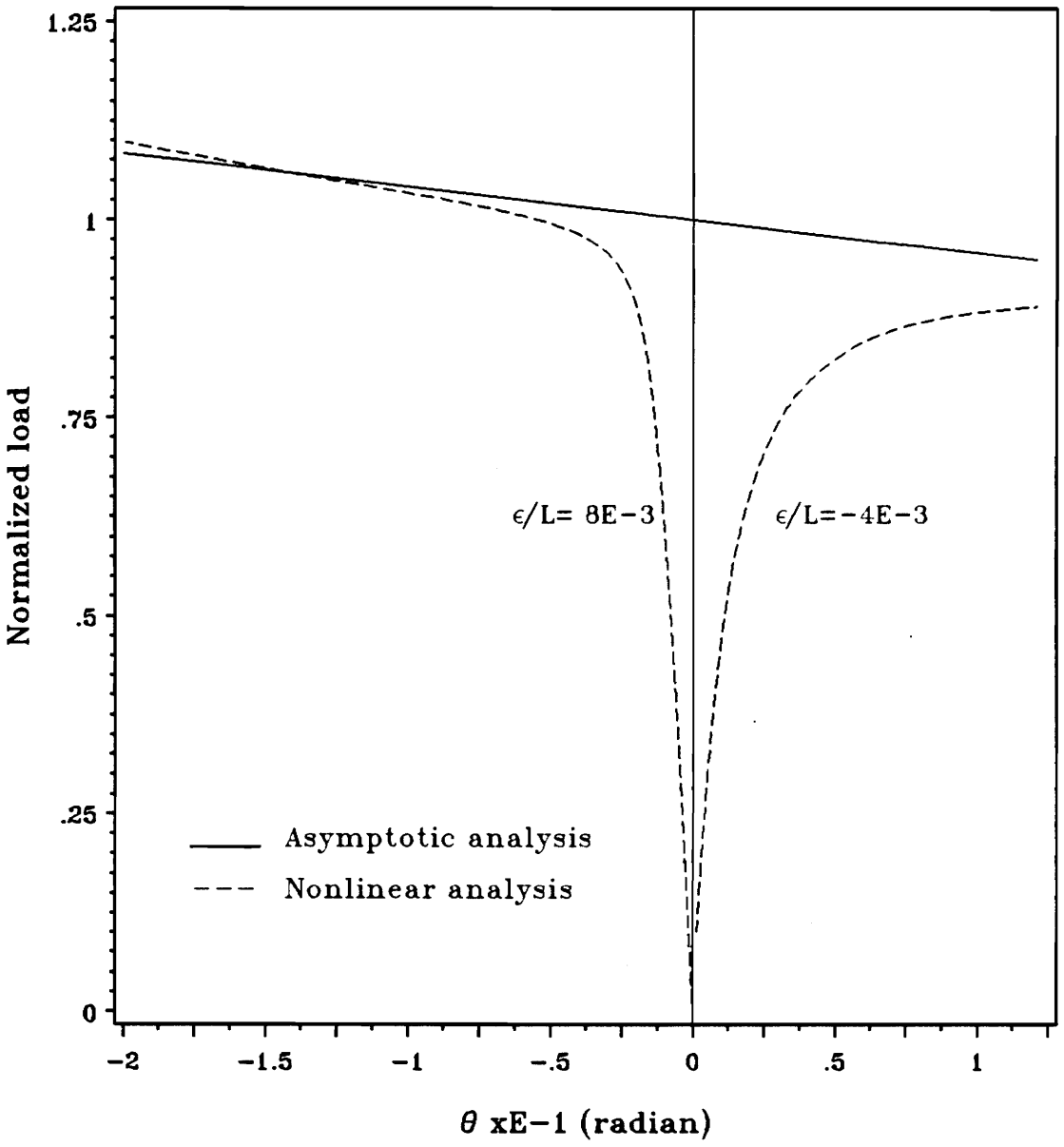

Figure 11. Load-displacement behavior for knee truss

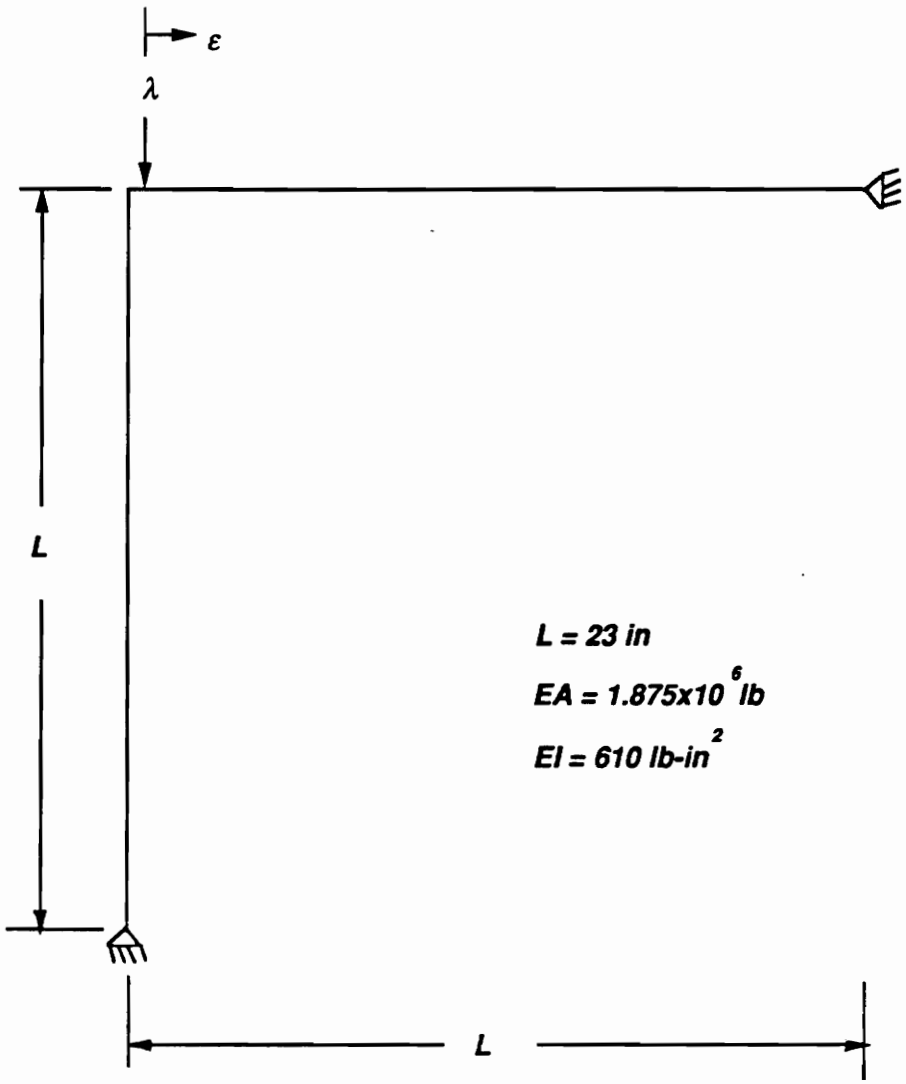

Figure 12. Knee frame

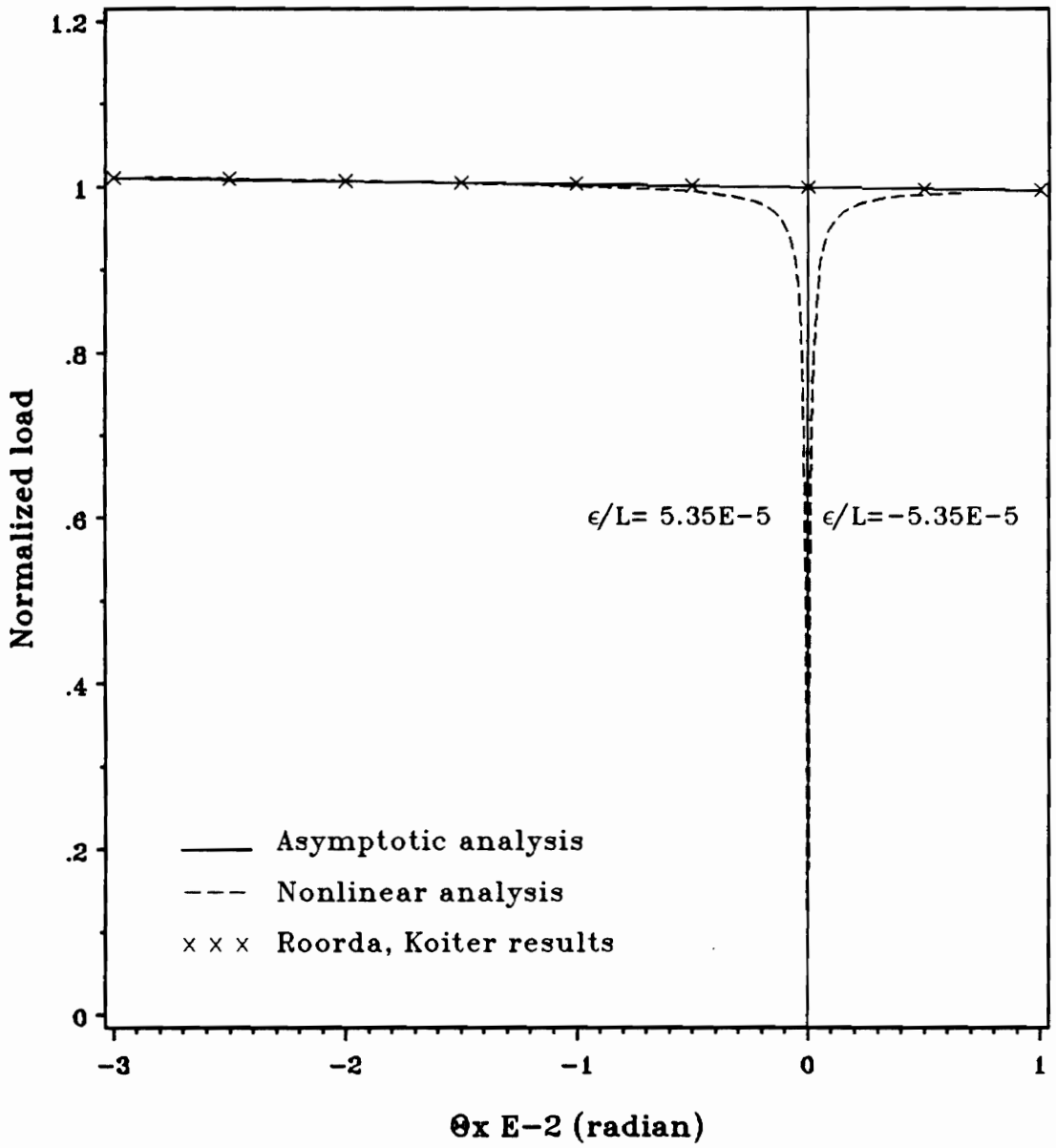

Figure 13. Load-displacement behavior for knee frame

List of References

1. Koiter, W.T., "On the stability of elastic equilibrium", Ph.D. Thesis, Polytechnic Institute, Delft, 1945, NASA (translation) TT F-10. 833, 1967.

2. Thompson, J.M.T., "Discrete branching points in the general theory of elastic stability", Journal of the Mechanics and Physics of Solids, Vol. 13, 1965, pp. 295 - 310.

3. Haftka, R.T., Mallett, R.H. and Nachbar, W., "A Koiter-type method for finite element analysis of nonlinear structural behavior", Technical Report AFFDL-TR-70-130, Vol. I, AFFDL-AFSC-W-PAFB, Ohio, 1970.

4. Haftka, R.T., Mallett, R.H. and Nachbar, W., "Adaption of Koiter's method to finite element analysis of snap-through buckling behavior", International Journal of Solids and Structures, Vol. 7, 1971, pp. 1427 - 1445.

5. Sewell, M.J., "The static perturbation technique in buckling problems", Journal of the Mechanics and Physics of Solids, Vol. 13, 1965, pp. 247 - 266.

6. Sewell, M.J., "A method of post-buckling analysis", Journal of the Mechanics and Physics of Solids, Vol. 17, 1969, pp. 219 - 234.

7. Budiansky, B. and Hutchinson, J.W., "Dynamic buckling of imperfection sensitive structures", Proceedings of the XI International Congress of Applied Mechanics, edited by Gortler, H., Springer-Verlag, 1964, pp. 83 - 106.

8. Hutchinson, J.W., "Imperfection sensitivity of externally pressurized spherical shells", Journal of Applied Mechanics, March 1967, pp. 49 - 55.

9. Thompson, J.M.T., "The branching analysis of perfect and imperfect discrete structural systems", Journal of the Mechanics and Physics of Solids, Vol. 17, 1969, pp. 1 - 10.

10. Budiansky, B., "Post-buckling behavior of cylinders in torsion", Theory of Thin Shells, IUTAM II Symposium, Copenhagen, September 1967, edited by Niordson, F.I., Springer- Verlag, 1969, pp. 212 - 233.

11. Carnoy, E.G., "Asymptotic study of the elastic post-buckling behavior of structures by the finite element method", Computer Methods in Applied Mechanics and Engineering, Vol. 29, November 1981, pp. 147 - 173.

12. Koiter, W.T., "Elastic stability and post-buckling behavior", Nonlinear Problems, Proceedings of a Symposium Conducted by the Mathematics Research Center, United States Army, University of Wisconsin, Madison, April 30 - May 2, 1962, edited by Langer, R.E., The University of Wisconsin Press, 1963, pp. 257 - 275.

13. Koiter, W.T., "Post-bucklig analysis of a simple two-bar frame", Recent Progress in Applied Mechanics, The Folke Odqvist Volume, edited by Broberg, B., Hult, J. and Niordson, F., John Wiley and Sons, 1967, pp. 337 - 354.

14. Haftka, R.T. and Nachbar, W., "Post-buckling analysis of an elastically-restrained column", International Journal of Solids and Structures, Vol. 6, 1970, pp. 1433 - 1449.

15. Hutchinson, J.W., "Initial post-buckling behavior of toroidal shell segments", International Journal of Solids and Structures, Vol. 3, 1967, pp. 97 - 115.

16. El Naschie, M.S., "Exact asymptotic solution for the initial post-buckling of a strut on linear elastic foundation", Zeitschrift fuer angewandte Mathematik und Mechanik, Vol. 54, 1974, pp. 677 - 683.

17. Di Carlo, A., Pignataro, M. and D'Asdia, P., "A modified potential approach to post-buckling analysis of frames ", Zeitschrift fuer angewandte Mathematik und Mechanik, Vol. 58, 1978, pp. T137 - T139.

18. Casciaro, R. and Aristodemo, M., "Perturbation approach to nonlinear post-buckling analysis", Zeitschrift fuer angewandte Mathematik und Mechanik, Vol. 58, 1978, pp. T139 - T141.

19. Roorda, J., "Stability of structures with small imperfections", Journal of the Engineering Mechanics Division, ASCE, Vol. 91, No. EM1, February 1965, pp. 87 - 106.

20. Roorda, J., "The buckling behavior of imperfect structural systems", Journal of the Mechanics and Physics of Solids, Vol. 13, 1965, pp. 267 - 280.

21. Roorda, J., "On the buckling of symmetric structural systems with first and second order imperfections", International Journal of Solids and Structures, Vol. 4, 1968, pp. 1137 - 1148.

22. Roorda, J. and Chilver, A.H., "Frame buckling: an illustration of the perturbation technique", International Journal of Non-Linear Mechanics, Vol. 5, 1970, pp. 247 - 258.

23. Lang, T.E., "Post-buckling of structures using the finite element method", Ph. D. Thesis, Dept. of Civil Engineering, University of Washington, Seattle, 1969.

24. Whetstone, W.D., EISI EAL Engineering Language Reference Manual, EISI - EAL System Level 2091, Engineering Information Systems Inc., July 1983.

25. Simitses, G.J., "An introduction to the elastic stability of structures", R. E. Krieger Pub. Co., 1986.

26. Croll, J.G.A. and Walker, A.C., "Elements of Structural Stability", John Wiley and Sons, 1972.

27. Mallett, R.H. and Marcal, P.V., "Finite element analysis of nonlinear structures", Journal of the Structural Division, ASCE, Vol. 94, No. ST9, September 1968, pp. 2081 - 2105.

28. Rajasekaran, S. and Murray, D.W., "Incremental finite element matrices", Journal of Structural Division, ASCE, Vol. 99, No. ST12, December 1973, pp. 2423 - 2438.

Vita

The author was born on November 10, 1966 in Bombay, India. He received his B. Tech degree in Aeronautical Engineering from I.I.T., Bombay in June 1988. In order to pursue higher studies he enrolled in the M.S. program in Aerospace Engineering at Virginia Tech. The author has accepted an engineering position at Engineering Analysis Services, Inc., Auburn Hills, MI.